



## **Pretreatment with erythropoietin of stem cell therapy in cyclosporine A induced nephrotoxicity: Histological, biochemical and pharmacological study**

Marwa Omar Abdl El All<sup>1</sup>, Mohamed M Khamiss Abd Elguaad<sup>2</sup>, Fatma A. Ahmed<sup>3</sup>, Heba Hussein Rohym<sup>4</sup>, Asmaa Mohammed Mohammed Ibrahim<sup>5</sup>, Radwa Mohammed Ahmed<sup>6</sup>, Ayman Mohamed Helal<sup>7</sup>

<sup>1</sup>Lecturer, Histology Department, Faculty of Medicine, Fayoum University, Egypt

<sup>2</sup>Lecturer, Physiology Department, Faculty of Medicine, Fayoum University, Egypt

<sup>3</sup>Lecturer, Medical Microbiology and Immunology Department, Faculty of Medicine, Fayoum University, Egypt

<sup>4</sup>Lecturer, Forensic Medicine and Clinical Toxicology Department, Faculty of Medicine, Fayoum University, Egypt

<sup>5</sup>Lecturer, Biochemistry and Molecular Biology Department, Faculty of Medicine, Fayoum University, Egypt

<sup>6</sup>Lecturer, Anatomy and Embryology Department, Faculty of Medicine, Fayoum University, Egypt

<sup>7</sup>Pharmacology Department, Faculty of Medicine, Fayoum University, Egypt

**Abstract:** Background: Cyclosporine A is one of the most commonly used immunosuppressant drugs in transplantation medicine in order to prevent graft rejection. However, it is highly toxic drug especially to kidney and pancreas. Stem cell therapy especially if preceded by erythropoietin administration could improve the adverse effects of cyclosporine A found to occur in renal tissue. **Aim of work:** is to elucidate the therapeutic effect of stem cells, especially pre-treated with erythropoietin, on cyclosporine A - induced nephrotoxicity in adult male albino rat and to demonstrate the limited role of spontaneous recovery in renal tissue repair. **Material and methods:** This research uses fifty adult male albino rats weighing 180-220 g. Ten rats were divided into five groups each: Group I (Normal control): The rats received olive oil at a dose of 1 ml/kg/ day subcutaneously once daily for one month. Group II (Cyclosporine A administration): The rats received cyclosporine A. Group III (Cyclosporine A administration with spontaneous recovery): The rats received cyclosporine A and left for a month following the last dose of Cyclosporine A for spontaneous recovery. Group IV (Cyclosporine A and stem cells administration): The rats received cyclosporine A. Stem cells were injected intravenously (dose:  $1 \times 10^6$  stem cells labelled with PKH26 dye in 1 ml phosphate buffer saline into the tail vein) 24 hours following the last dose of cyclosporine A. Group V (Cyclosporine A, stem cells with erythropoietin pre-administration): The rats received cyclosporine A. Stem cells were injected intravenously 24 hours following the last dose of cyclosporine A. 48 hours before stem cell therapy, rats were injected intravenously, into the tail vein, with 1 ml of erythropoietin. The dose of cyclosporine A 15 mg/kg/ day subcutaneously once daily for one month. Rats of groups I, II were sacrificed after one month, III, IV and V after two months. The kidneys were removed and processed for histological and biochemical studies. **Results:** Light microscopic examination of rat kidney specimens, of rats the received cyclosporine A, stained with haematoxylin and eosin showed extensive degeneration of lining epithelial cells in renal cortex and medulla, cytoplasmic vacuolation, and haemorrhage. Treatment with mesenchymal stem cells, especially pre-treated with erythropoietin greatly ameliorated these histological alterations much more than the effect of spontaneous recovery. [Marwa Omar Abdl El All, Mohamed M Khamiss Abd Elguaad, Fatma A. Ahmed, Heba Hussein Rohym, Asmaa Mohammed Mohammed Ibrahim, Radwa Mohammed Ahmed, Ayman Mohamed Helal. **Pretreatment with erythropoietin of stem cell therapy in cyclosporine A induced nephrotoxicity: Histological, biochemical and pharmacological study.** *J Am Sci* 2020;16(9):10-32]. ISSN 1545-1003 (print); ISSN 2375-7264 (online). <http://www.jofamericanscience.org>. 2. doi:[10.7537/marsjas160920.02](https://doi.org/10.7537/marsjas160920.02).

**Keywords:** Cyclosporine A, stem cells, erythropoietin, kidney.

### **1. Introduction:**

Cyclosporine A (CsA) is a commonly used immunosuppressive drug which makes it an appealing immunosuppressive medication in solid organ transplantation and autoimmune diseases due to its immunological properties. However, it induces acute or chronic nephrotoxicity with subsequent histopathological alterations in renal tissue and kidney function impairment (1).

CsA possesses several other side effects such as hyperkalemia, hypomagnesaemia, hyperuricemia,

hypertension, hyperlipidemia, gingival hyperplasia, neurotoxicity, and thrombotic microangiopathy. Nephrotoxicity of CsA causes renal failure arising from renal vasoconstriction, tubular injury and atrophy, interstitial fibrosis, and glomerular sclerosis. Clinical and experimental studies have shown that nephrotoxicity pathogenesis caused by CsA may involve multiple factors. It has been shown that CsA stimulates the renin-angiotensin system (RAS),

generates reactive oxygen species and upregulates the expression of the Transforming growth factor beta 1 (TGF- $\beta$ 1). TGF- $\beta$ 1 is playing a major role in renal fibrosis pathogenesis; dose-dependent increases in TGF- $\beta$ 1 expression have been reported to be associated with CsA administration. RAS activation contributes to the nephrotoxicity of the inhibitors of calcineurin because of its vasoconstrictive, pro-inflammatory and pro-fibrogenic effects (2,3,4).

Mesenchymal stem cell (MSC) transplantation can decrease drug-induced nephropathy. MSCs are adherent, fibroblast-like cells, of various tissues and organs like the blood of the umbilical cord, bone marrow, adipose tissue, lung, heart, and other organs (5,6). MSCs are multipotent cells that could proliferate and differentiating into adipocytes, osteoblasts and chondrocytes. They are involved in cell therapy and tissue regeneration because of their regenerative and immunomodulatory properties. Injections of MSCs or microvesicles (MVs) extracted from MSCs were studied for various diseases and most of these procedures were also confirmed in clinical studies (7,8,9).

MSCs affect both acute and chronic nephropathy with protective effects. The Defence appears to be associated to immunomodulation, anti-apoptotic impact, and inflammation and fibrosis reduction (10,11).

MSCs therapy's major adverse effects are A lack of clear homing following systemic infusion and premature deaths of injected cells due to micro-environmental injury with several factors, including local hypoxia, oxidative stress, and inflammation, which could decrease the efficacy of MSCs. Applying pretreated or updated MSCs is a modern technique for improving MSCs' ability to migrate and strengthen tissue healing for treating kidney injury. Pretreatment or modifying by cytokines such as insulin growth factor 1, hypoxia-inducible factor-1 $\alpha$ , and heme oxygenase- 1 before infusion, can boost the amount of MSCs that homes the injured kidney, enhance renal function recovery, and ameliorate renal histopathological impairment (12,13). Pretreatment with erythropoietin before administration of MSCs may obtain similar results. Some experimental in vitro studies showed that EPO gene-transfection overexpression in MSCs can further improve the preventive role on neural harm caused by hypoxia. In addition, some findings indicated that increased proliferation and migration of MSCs could be related to EPO gene modification (14,15).

## 2. Material and methods:

### Chemicals: 1- Cyclosporine A:

It was acquired by Novartis Pharmaceuticals Corporation (East Hanover, New Jersey, USA) in the

form of 25mg containing capsules that were dissolved in olive oil to obtain a final concentration of and were injected subcutaneously once daily for four weeks (16).

**2- Erythropoietin:** was available in an injectable human recombinant erythropoietin supplied by the Egyptian Pharmex Company (10000 IU/ml) Shenyang Sunshine Pharmaceutical Co., China. It was given once at a dose of 0.5 ml intravenously into the tail vein (1).

**3- Stem cells: Bone marrow (BM) - derived mesenchymal stem cells (MSC):** Received from the stem cell research unit at the Department of Biochemistry of Kasr Al Aini, Faculty of Medicine, University of Cairo. PKH26, red fluorescent cell linker mini kit for general cell membrane labeling (Sigma Aldrich, USA), Sigma brand, catalog number: MINI 26. It's in the form of PKH26 dye stock solution (1 vial containing 0.1 ml, 1x 10<sup>-3</sup> M in ethanol) and diluent C (1 vial containing 10 ml). This dye has been used in group IV. Stem cell dose: 1x10<sup>6</sup> PKH26 dye marked stem cells in 1 ml of saline phosphate buffer (PBS) into the tail vein, **Rats of this group** received stem cells at 24 hours following the last dose of Cyclosporine A (17).

**Animals:** This study utilized fifty adult male albino rats weighing 180-220 g. They have been collected from the house of animal, Faculty of Medicine, University of Cairo. The rats were lodged in individual cages and fed with standard rat chow under standard laboratory and environmental conditions. The rats were split into five groups each with 10 rats:

**Group I (Normal control):** This group of rats received 1 ml/kg/day of olive oil subcutaneously once daily for one month.

**Group II (Cyclosporine A administration group):** This group of rats received cyclosporine A subcutaneously at 15 mg / kg / day dose once daily for one month.

**Group III (Cyclosporine A administration with spontaneous recovery):** This group of rats received cyclosporine A subcutaneously at 15 mg / kg / day dose once daily for one month and left for a month following the last dose of Cyclosporine A for spontaneous recovery.

**Group IV (Cyclosporine A and stem cells administration group):** This group of rats received cyclosporine A subcutaneously at 15 mg / kg / day dose once daily for one month. Stem cells were injected intravenously (dose: 1x10<sup>6</sup> PKH26 dye marked stem cells in 1 ml of saline phosphate buffer into the tail vein) 24 hours following the last dose of cyclosporine A.

**Group V (Cyclosporine A, stem cells with erythropoietin pre-administration group):** This group of rats received cyclosporine A subcutaneously

at 15 mg / kg / day dose once daily for one month. Stem cells were injected intravenously (dose:  $1 \times 10^6$  PKH26 dye marked stem cells in 1 ml of saline phosphate buffer into the tail vein) 24 hours following the last dose of cyclosporine A. 48 hours before stem cell therapy, rats were injected intravenously, into the tail vein, with 1 ml of erythropoietin.

Rats of groups **I**, **II** were sacrificed after one month, **III**, **IV** and **V** after two months. The kidneys were removed and processed for histological and biochemical studies.

#### Methods:

The kidneys were excised and processed for the following studies:

1-Light microscopic study using hematoxylin and eosin stain (**18**): The renal tissues were fixed in 4% paraformaldehyde. The histological sections in xylene were deparaffinized, rehydrated via a graded ethanol series, and washed in running water. The sections were then submerged for two minutes in Harris' hematoxylin, washed in running water (five minutes), rinsed in distilled water (one minute), stained in an aqueous eosin solution (five minutes), and dehydrated in upward ethanol concentrations. The sections were then cleared in xylene (three successive changes, one minute each) and placed under a coverslip.

2-Electron microscopic examination (**19**): From each section of the equatorial muscle, small cylinders (4 mm long x 1 mm x 1 mm) of tissue were prepared. These samples of kidney tissue were fixed at 4 ° C for 48 h by immersion in vials containing 1 mL of mixed solution glutaraldehyde 1.25% and paraformaldehyde 1% in a buffer solution of phosphate-buffered saline (PBS). Samples were washed for 45 min using PBS 0.14 M (pH = 7.4). Repeated this process three times. Consequent steps were taken by the Universitat de Barcelona Serveis Científico-Tècnics (SCT). In the SCT, samples in osmium tetroxide (OsO<sub>4</sub>) were subjected to a 1 % post-fixation process in PBS for 1 h. They then dehydrated samples in acetone. They had been left for 10 min in various solutions with increasing concentrations of acetone. Dehydrated samples were mounted on resin blocks of Spurr's epoxide. The resin blocks have been cut and semithin sections (1.5µm) handled. Then these sections were observed at 40× with an optic microscope to pick to choose the regions of interest for analyzing and processing using TEM. The regions selected were cut and inserted into square and eyelet grids. They were contrasted in order to be able to study with TEM.

3- Immunofluorescence study:

#### Detection of stem cells using fluorescence microscopy:

This is the most suitable method for long-term detection of human MSC in vitro and in vivo. MSC

were fluorescently labeled and detected by fluorescence microscopy expressing red fluorescence protein.

#### Isolation of BM-derived MSC from rats (20):

Bone marrow was extracted by flushing adult male rats' tibia and femurs with Dulbecco's modified Eagle's medium (DMEM, GIBCO/BRL) complemented with 10% foetal bovine medium (GIBCO/BRL). Nucleated cells have been isolated with a gradient of density [Ficol / Paque (Pharmacia)] and suspended with 1 % penicillin- streptomycin (GIBCO / BRL) in a full culture medium.

Cells were incubated as primary culture at (37<sup>o</sup> C) for 12-14 days in 5 % humidified Co<sub>2</sub> or when large colonies were formed. As large colonies formed (80-90% confluence), cultures were washed twice with phosphate buffer saline (PBS) and cells were trypsinized for 5 minutes at (37<sup>o</sup> C) with 0.25% trypsin in one ml ethylenediaminetetraacetic acid (EDTA) (GIBCO / BRL). Cells were resuspended with serum-supplemented medium after centrifugation (at 2400 rpm for 20 minutes) and incubated in a 50 cm<sup>2</sup> Falcon culture flask. The resultant cultures have been referred to as cultures of first-passage.

#### Morphological identification of BM- derived MSC:

In culture, MSC was characterized by its adhesively and fusiform shape and by the detection of CD29, one of the surface markers of mesenchymal stem cells in rats (**21**).

#### Labeling of stem cells with PKH26 dye:

During the 4th passage, MSC was collected and labeled with PKH26 fluorescence linker dye. PKH26 is a red fluorochrome with an excitation (551 nm) and an emission (567 nm). The linkers are stable physiologically, showing little to no toxic side -effects on cell systems. Labeled cells maintain both biological activity and proliferation, and are suitable for in vitro cell labeling, in vitro proliferation studies and long term, in vivo cell tracking. For non-dividing cells, labeled cells that have been washed up to 100 days after staining may be visualized in culture. This enhanced stability is beneficial for in vivo studies in the long term. The dye itself is stable and will split evenly when the cells divide apart. After staining with PKH dyes, depending on how brightly the cells were initially stained and the amount of surface area on the cells, one can observe as many as eight divisions. Most generally, one can imagine 4-6 divisions.

#### Components of PKH26 Red Fluorescent Cell Linker Kit (Sigma-Aldrich):

- PKH26 dye stock (one vial containing >0.1 ml,  $1 \times 10^{-3}$  M in ethanol)
- Diluent C (an iso-osmotic aqueous solution that does not contain physiological salts or buffers, detergents, or organic solvents and is engineered to preserve cell viability while improving dye solubility)

and staining effectiveness, one vial containing > 10 ml).

#### Steps of labeling cells with PKH26 dye

Final concentration of  $2 \times 10^{-6}$  M PKH26 dye and  $1 \times 10^7$  cells/ml in a 2 ml total volume was stained according to the following aseptic techniques according to (Sigma Protocol):

1) Proteolytic enzymes (i.e., trypsin) were used to remove adherent or bound cells and placed into a single cell suspension.

2) All procedures were completed at  $25^{\circ}$  C. A total volume of approximately  $2 \times 10^7$  single cells was put in a conical polypropylene tube at the bottom and was washed without serum once using culture medium.

3) The cells were centrifuged (400 x g) into a loose pellet for 5 minutes.

4) The supernatant was carefully aspirated after centrifuging cells leaving no more than 25 ml of supernatant on the pellet.

5) One ml of diluents C was added. Cells were suspended, pipetting to insure complete dispersion was done.

6) Immediately before staining,  $4 \times 10^{-6}$  molar PKH26 dye (this will be a 2X stock) was prepared in polypropylene tubes using diluent C (supplied with the kit). To reduce the impact of ethanol, the amount of dye added was less than 1% of the individual sample volume.

7) The one ml of 2X cells was rapidly added to one ml of 2X dye and the sample was immediately mixed by pipetting (rapid and homogenous mixing was critical for uniform labeling because staining is nearly instantaneous).

8) The sample was incubated 4 minutes at  $25^{\circ}$  C. During this staining period, the tube was periodically gently inverted to ensure mixing at  $25^{\circ}$  C.

9) The staining reaction was halted by the addition of an equivalent amount of serum and was incubated for one minute.

10) The serum-stopped sample was diluted with an equal volume of complete medium (not diluents C).

11) For the removal of cells from the staining solution, the cells were centrifuged at 400 X g for 10 minutes at  $25^{\circ}$  C.

12) The supernatant was removed and the pellet was transferred to a new tube for further washing (at least three washes were recommended).

13) To wash the cells, 10 ml of a full culture medium was added and the cells were centrifuged and resuspended to the desired concentration.

14) Fluorescence microscopy was used to examine the cells (**Sigma-Aldrich, Saint Louis, USA**).

4-Biochemical study: assessment of levels of:

a- serum creatinine and blood urea nitrogen (**BUN**):

Measurement of Creatinin Concentration (**22**): Collected blood was store at microtube 1.5 mL without anticoagulant then be sentrifuged at 5000 rpm for 5 minutes. Serum was transfered to other microtubes before analyzed. Fifty microliter of collected serum was added to 1000  $\mu$ L monoreagent from Diasys creatinin measuring kit and incubated for 60 seconds. The absorbance of serum samples were read at  $\lambda$  492 nm twice with interval 1 minute. The first absorbance of serum samples was averaged with the second absorbance and multiplied with multiplier which printed on Diasys creatinin measuring kit.

Measurement of **BUN (23)**: was evaluated by automated validated methods on a Hitachi 717 analyser (Roche Diagnostics Inc, Mass USA).

b-Oxidative stress: Superoxide dismutase (**SOD**), glutathione peroxidase (GSH) and renal thiobarbituric acid (RTAB) (**24**):

Rat kidneys were rapidly thawed and manually homogenized in cold phosphate buffer (0.1 mmol/lit, pH 7.4, containing 5mmol/lit EDTA) and debris removed by centrifugation at 2000 g for 10 min (Centrifuge 5415 R; Rotofix 32A, Germany). Supernatants were recovered and used for protein measurement, lipid peroxidation value, antioxidant enzyme activities, and GSH-content. Protein content of kidneys supernatants was determined using a colorimetric method of Lowry with bovine serum albumin as a standard.

#### Measurement of SOD activity

Superoxide dismutase (SOD) activity was assessed with the Randox SOD detection kit as per the manufacturer's instructions. SOD's function is to accelerate the dismutation of the toxic superoxide ( $O_2^-$ ) produced to hydrogen peroxide and molecular oxygen during oxidative energy processes. This method uses xanthine and xanthine oxidase to produce superoxide radicals that react to form a red formazan dye with 2-(4-iodophenyl)-3-(4-nitrophenol)-5-phenyltetrazolium chloride (I.N.T). The SOD activity is then calculated by degree to which this reaction is inhibited. One unit of SOD is that which under assay conditions induces 50 % inhibition of the rate of INT reduction. SOD levels were recorded via a standard curve at 505 nm and expressed as unit per milligram of tissue protein (unit/mg protein).

#### Measurement of GSH activity

According to manufacturer's instructions, glutathione peroxidase (GSH) activity was assessed with the Randox GSH detection kit. GSH catalyse the oxidation of glutathione by cumene hydroperoxide. The oxidized glutathione (GSSG) is rapidly converted to the reduced form with a concomitant oxidation of NADPH to NADP<sup>+</sup> in the presence of glutathione

reductase (GR) and NADPH. The absorbance decrease was measured spectrophotometrically (S2000 UV model; WPA, Cambridge, UK) against blank at 340 nm. One unit (U) of GSH was defined as 1  $\mu$ mol of oxidized NADPH per min per milligram of tissue protein. The GSH activity was expressed as unit of tissue protein per milligram (unit/mg protein).

The content of the thiobarbituric acid reactive substances (TBARS) in the kidney indicated the concentration of lipid peroxidation. Tissue TBARS determined by following the production of thiobarbituric acid reactive substances. In brief, 40  $\mu$ l of supernatant was applied to 40  $\mu$ l of 0.9% NaCl and 40  $\mu$ l of deionized H<sub>2</sub>O, which resulted in a total reaction volume of 120  $\mu$ l. The reaction was incubated for 20 min at 37° C for 20 min and halted by adding of 600  $\mu$ l of cold 0.8 mol/l hydrochloride acid, comprising 12.5% trichloroacetic acid. After adding 780  $\mu$ l of 1 % TBA, the reaction was boiled for 20 minutes and then cooled for 1 h. at 4° C. The cooled reaction was spun at 1500 g in a microcentrifuge for 20 min to measure the amount of TBARS formed by the homogenate, and the absorbance of the supernatant was read spectrophotometrically at 532 nm using an extinction coefficient of  $1.56 \times 10^5$  /M.Cm. For all the TBARS assays, the blanks contained an additional 40  $\mu$ l of 0.9 % NaCl instead of the homogenate one just mentioned. The results of TBARS were expressed as nmol per milligram of tissue protein (nmol/mg protein).

**5- PCR analysis of: a-Interleukin 1 beta (IL1b): (25,26):** Real-Time Quantitative PCR Analysis: The mRNA concentrations of **IL1-b** and  $\beta$ -actin in the rat kidney specimens were quantified by quantitative real-time PCR.  $\beta$ -actin was used as a housekeeping gene to normalize the gene expression data. The primer information for all the genes is: Sequences for real-time PCR primers.

**$\beta$ -Actin** : ACCGCAAATGCTTCTAAACC  
ATAAAGCCATGCCAATCTCG

**IL-1 $\beta$** : TCTTACC GCCTGGACACG  
TAGTGGCGATGTTGACCTG

Total RNA was obtained using TRIzol reagent (Invitrogen, Carlsbad, CA, USA) according to the manufacturer's protocol, and the RNA integrity was assessed via 1% agarose gel electrophoresis. The RNA concentrations and purity were determined from OD<sub>260</sub>/OD<sub>280</sub> readings (ratio >1.8) using a NanoDrop ND-1000 spectrophotometer (NanoDrop Technologies, Wilmington, DE) and adjusted to the same concentration. The RNA was reverse transcribed to cDNA by using a PrimeScript RT reagent kit (Takara, Shiga, Japan). Real-time quantitative PCR was carried out in a 7500 Real-Time PCR system (Applied Biosystems, Foster City, CA, USA) using a SYBR Green PCR kit (Roche Diagnostics, Laval,

Quebec, Canada). All samples were analyzed in triplicate, and the results were expressed as  $2^{-\Delta\Delta CT}$ . Each cycle consisted of denaturation at 95°C for 10 s, annealing at 95°C for 5 s, and extension at 60°C for 34 s. Each sample was measured in triplicate, and the average values were obtained.

b-Vascular endothelial growth factor (VEGF): **Real-time Quantitative RT-PCR (RT-qPCR) (27, 28):** Total RNA was purified using the RNeasy mini kit (Qiagen, Valencia, CA), and cDNA was synthesized using the iScriptc DNA synthesis kit (Bio-Rad) with 0.5  $\mu$ g of total RNA according to the manufacturer's recommendations. qPCR was performed with primers specific for VEGF, and GAPDH using iQ SYBR Green Supermix in an iQ5 real-time PCR detection system (Bio-Rad). The primers were designed and ordered from Integrated DNA Technologies (Coralville, IA), and primer sequences used were as follows: VEGF, 5\_-GTTCAGTGTGAGCCTTGTTTCAG-3\_ (forward) and 5\_-GTCACATCTGCAAGTACGTTTCG-3\_ (reverse); and GAPDH, 5\_-CTGGAGAAACCTGCCAAGTA-3\_ (forward) and 5\_-TGTTGCTGTAGCCGATTCA-3\_ (reverse). Pilot real-time RT-qPCR experiments were performed to determine optimal condition for each primer. All real-time RT- qPCR experiments were performed in duplicate. The primer specificity of the amplification product was confirmed by melting curve analysis of the reaction products using SYBR Green as well as by visualization on ethidium bromide-stained agarose (1.5%) gels. The housekeeping gene GAPDH was used as an internal control, and gene-specific mRNA expression was normalized against GAPDH expression. iQTM5 optical system software (Bio-Rad; version 2.0) was used to analyze real-time RT-qPCR data and derive threshold cycle (CT) values according to the manufacturer's instructions.

c-Caspase 3 d-Transforming growth factor beta 1 (TGF-b1): **Analysis of mRNA expression by real time polymerase chain reaction (RT-PCR) of Caspase 3 and TGF-b1:** Quantitative real-time PCR was performed using a SYBR PrimeScript mRNA RT-PCR Kit and SYBR Premix Ex TaqII (Tli RNaseHPlus) (Takara, Japan) with the intron-spanning primers on ABI-Prism-7500 Sequence Detection System (Applied Biosystems, Waltham, MA). Reactions were performed in triplicate and the specificity was monitored using the melting curve analysis after the total cycling. The relative mRNA of **Caspase 3 and TGF- $\beta$ 1** were quantified using the  $2^{-\Delta\Delta CT}$  method. The sequences of the PCR primers are:

**Caspase 3-forward-**  
GATACCGGTGGAGGCTGACT, **reverse-**  
TGCCACCTTCCTGTAAACGC. **TGF- $\beta$ 1-forward-**

CCTATTCCGGACCAGCCCTC, reverse-  
ATAGGGGAGCTACTGCCAGC.

### Results: Histological results:

**Group I (Normal control):** Light microscopic examination of haematoxylin stained renal cortex and eosin stain revealed renal corpuscles, composed of a dense, round glomerulus enclosed with the aid of using a parietal layer of Bowman's tablet with the urinary area in-between. Proximal convoluted tubules are lined with low columnar cells with strongly acidophilic cytoplasm and spherical basal nuclei. Low cuboidal cells with faint acidophilic cytoplasm and rounded central nuclei are lined with the distal convoluted tubules. An intact apical brush border of proximal and distal convoluted tubule could be observed (Figs.1,2).

Electron microscopic examination of renal cortex of the same group showed a proximal convoluted tubular cell with heterochromatic nucleus with prominent nucleolus and intact nuclear envelope, there is an abundance of parallel electron dense mitochondria among the nucleus and a uniformly skinny basal cell membrane, intact basal infoldings and intact apical microvilli (Figs.3,4).

Examination of the renal medulla stained with haematoxylin & eosin presented the collection of tubules coated with easy columnar epithelium and Henle loops coated with easy cuboidal epithelium with scanty cytoplasm and a bulging lumen nucleus (Fig. 5)

Electron microscopic examination of renal medulla of the same group revealed Henle's epithelial lining cell has a medullary thick ascending limb with a heterochromatic nucleus with an outstanding nucleus associated an intact nuclear envelope, basal introversion, a uniformly skinny basal cell wall and associate abundance of dense electron mitochondria with intact cristae and intact apical microvilli (Figs.6,7).

### Group II (Cyclosporine A administration):

Light microscopic examination of haematoxylin stained renal cortex and eosin stain showed extremely shrunken glomeruli with widened in-between urinary area. Most of proximal and distal convoluted tubules exhibited extensive fat degeneration, cytoplasmic vacuolation and exfoliation of lining epithelial cells lost apical brush border, intra-luminal casts, with pyknotic, karyolytic nuclei. The interstitial tissue featured areas of hyaline degeneration, haemorrhage and mononuclear cell infiltration (Figs. 8, 9)

Electron microscopic examination of renal cortex of the same group showed a proximal convoluted tubular cell with extremely shrunken or karyolytic nucleus with clumped chromatin and indented nuclear envelope, extensive cytoplasmic rarefaction, ballooned mitochondria with damaged cristae, lost apical

microvilli, and extremely thickened basal cell membrane. A macrophage could be observed in the interstitial tissue (Figs. 10, 11,12).

Examination of the renal medulla stained with haematoxylin & eosin presented Henle's loops and collecting tubules with intra-luminal casts, nuclear pyknosis, karyolysis, exfoliation of lining epithelial cells, cytoplasmic vacuolation and fat degeneration. The interstitial tissue featured areas of haemorrhage (Fig.13).

Electron microscopic examination of renal medulla of the same group revealed an epithelial coating cell with a medullary dense rising Henle limb with a degenerated nucleus with clumped chromatin, extensive cytoplasmic rarefaction ballooned mitochondria with damaged cristae and extremely thickened basal cell membrane (Fig.14).

### Group III (Cyclosporine A administration with spontaneous recovery):

Light microscopic examination of haematoxylin stained renal cortex and eosin stain showed extremely shrunken glomeruli with widened in-between urinary area. Most of proximal and distal convoluted tubules exhibited a lost border of the apical brush, intra-luminal casts, exfoliation of lining epithelial cells, cytoplasmic vacuolation, fat degeneration with pyknotic, karyolytic nuclei. The interstitial tissue featured few areas of hyaline degeneration (Fig.15).

Electron microscopic examination of renal cortex of the same group showed proximal convoluted tubular cells with a degenerated nucleus with clumped chromatin and indented nuclear envelope, pathological aggregation of ballooned mitochondria with damaged cristae or abundant mitochondria with intact cristae, partially damaged or intact apical microvilli, mild cytoplasmic rarefaction, moderately thickened basal cell membrane with intact basal infoldings (Figs.16,17).

Examination of the renal medulla stained with haematoxylin & eosin presented loops of Henle and collecting tubules with cytoplasmic vacuolation, karyolytic nuclei and exfoliation of lining epithelial cells. The interstitial tissue featured areas of hyaline degeneration, and mononuclear cell infiltration (Fig. 18).

Electron microscopic examination of renal medulla of the same group revealed an epithelial coating cell with a medullary dense rising Henle limb with a karyolytic nucleus with indented nuclear envelope intact mitochondria with intact cristae, partially damaged apical microvilli and thin basal cell membrane with intact basal infoldings (Fig. 19).

### Group IV (Cyclosporine A and stem cells administration):

MSCs labeled with PKH26 fluorescent dye detected in this group, confirmed homing of these cells into the renal tissue (**Fig. 20**).

Light microscopic examination of haematoxylin treated renal cortex and eosin stain revealed almost normal glomeruli enclosed with the aid of using a parietal layer of Bowman's tablet with the urinary area in-between. Some proximal and distal convoluted tubules show intact apical brush border but few of them displayed intra-luminal casts and exfoliation of lining epithelial cells (**Fig. 21**).

Electron microscopic examination of renal cortex of the same group showed a proximal convoluted tubular cell with a heterochromatic nucleus with prominent nucleolus and intact nuclear envelop or degenerated nucleus with clumped chromatin, intact apical microvilli, intact basal infoldings and abundant intact mitochondria with intact cristae but few of them are ballooned with damaged cristae (**Figs. 22, 23**).

Examination of the renal medulla stained with haematoxylin & eosin presented some loops of Henle and collecting tubules with cytoplasmic vacuolation, karyolytic nuclei, intra-luminal casts and exfoliation of lining epithelial cells. The interstitial tissue featured few areas of haemorrhage (**Fig. 24**). Electron microscopic examination of renal medulla of the same group revealed an epithelial lining cell with a medullary dense ascending Henle limb with an extremely karyolytic or degenerated nucleus with clumped chromatin, mild cytoplasmic rarefaction, ballooned mitochondria with damaged cristae, mildly thickened or thin basal cell membrane with lost basal infoldings and intact apical microvilli (**Figs. 25, 26**).

#### **Group V (Cyclosporine A, stem cells with erythropoietin pre-administration):**

MSCs labeled with PKH26 fluorescent dye detected in this group, confirmed homing of these cells into the renal tissue (**Fig. 27**). Light microscopic examination of haematoxylin stained renal cortex and eosin stain revealed apparently normal renal corpuscles, comprised of a thick rounded glomerulus enclosed by a parietal layer of Bowman's capsule with the urinary space in-between. Proximal convoluted tubules and distal convoluted tubules with intact apical brush border (**Fig. 28**). Electron microscopic examination of renal cortex of the same group showed an apparently normal proximal convoluted tubular cell with heterochromatic nucleus with prominent nucleolus and intact nuclear envelop (arrowhead), abundant parallel electron dense mitochondria and intact basal infoldings (**Fig. 29**).

Examination of the renal medulla stained with haematoxylin & eosin presented apparently normal loops of Henle and collecting tubules with mildly congested blood vessels in-between (**Fig. 30**). Electron microscopic examination of renal medulla of the same

group showed an apparently normal epithelial coating cell of medullary thick rising limb of Henle with heterochromatic nucleus with prominent nucleolus and intact nuclear envelop, basal infoldings and abundant electron dense mitochondria with intact cristae (**Fig. 31**).

#### **Statistical analysis of data:**

Using SPSS software statistical computer package version 22 (SPSS Inc, USA), the data collected were arranged, tabulated and statistically analysed. The estimate of the mean and standard deviation (SD). One way ANOVA (Variance Analysis) was used to analyse the difference of mean values of calculated variables between groups, multiple comparisons between pairs of groups were made using Tukey HSD (Post-hoc range test). Significance was adopted at  $P \leq 0.05$  for the interpretation of results of significant tests.

**SOD** was statistically significantly lower in group II ( $2.23 \pm 0.42$ ), III ( $2.62 \pm 1.11$ ), and IV ( $4.08 \pm 1.03$ ) when compared to control ( $6.99 \pm 1.29$ ),  $p < 0.0001$ . However, there was no substantial statistical difference between group V and control,  $p = 0.780$ . On the other hand, SOD was a statistically significantly higher in both groups; IV ( $4.08 \pm 1.03$ ) and V ( $6.29 \pm 0.77$ ) as compared to group II ( $2.23 \pm 0.42$ ),  $p = 0.048$  and  $p < 0.0001$ , respectively. But, there was no a statistically significantly difference between group III and group II,  $p = 0.966$ . Also, it was statistically significantly higher in group V ( $6.29 \pm 0.77$ ) as compared to group III ( $2.62 \pm 1.11$ ),  $p < 0.0001$ . However, the difference between group IV and III was not significant statistically,  $p = 0.166$ . Also, the difference has been statistically relevant between the group IV and group V ( $p = 0.014$ ) (**Figs. 32,33**).

Glutathione peroxidase was statistically significantly lower in group II ( $10.01 \pm 3.39$ ), III ( $11.87 \pm 3.61$ ), and IV ( $20.05 \pm 1.95$ ), when compared to control ( $29.76 \pm 4.33$ ),  $p < 0.0001$ ,  $p < 0.0001$  and  $p = 0.001$ , respectively. However, there was no a statistically significant difference between group V and control,  $p = 0.112$ . Also, Glutathione peroxidase was a statistically significantly lower in group IV ( $20.05 \pm 1.95$ ) and group V ( $24.30 \pm 2.95$ ) as compared to group II ( $10.01 \pm 3.39$ ),  $p = 0.001$  and  $p < 0.0001$ , respectively. There was, however, no statistically significant difference between group III ( $p = 0.900$ ) versus group II. Also, it was statistically significantly higher in group IV ( $20.05 \pm 1.95$ ) and group V ( $24.30 \pm 2.95$ ) as compared to group III ( $11.87 \pm 3.61$ ),  $p = 0.008$  and  $p < 0.0001$ , respectively. However, there was no a statistically significant difference between the group IV and group V ( $p = 0.294$ ) (**Figs. 34, 35**).

Renal thiobarbituric acid (RTBA) was statistically significantly higher in group II ( $4.66 \pm$

0.52), III ( $3.99 \pm 0.76$ ), and IV ( $3.30 \pm 0.47$ ) when compared to control ( $2.12 \pm 0.15$ ),  $p < 0.0001$ ,  $p < 0.0001$  and  $p = 0.041$ , respectively. However, there was no a statistically significant difference between group V and control,  $p = 0.588$ . On the other hand, RTAB was a statistically significantly lower in both groups; IV ( $3.30 \pm 0.47$ ) and V ( $2.59 \pm 0.42$ ) as compared to group II ( $4.66 \pm 0.52$ ),  $p = 0.003$  and  $p < 0.0001$ , respectively. But, there was no a statistically significant difference between group III and group II,  $p = 0.255$ . Also, it was statistically significantly lower in group V ( $2.59 \pm 0.42$ ) as compared to group III ( $3.99 \pm 0.76$ ),  $p = 0.002$ . However, the difference between group IV and III was not a statistically significant,  $p = 0.233$ . Also, no statistically significant difference was found between the group IV and group V ( $p = 0.219$ ) (Figs. 36,37).

**BUN** (mg/dl) was statistically significantly higher in group II ( $79.86 \pm 8.81$ ), III ( $59.51 \pm 7.96$ ), and IV ( $37.69 \pm 9.5$ ) when compared to control ( $18.20 \pm 2.14$ ),  $p < 0.0001$ ,  $p < 0.0001$  and  $p = 0.002$ , respectively. However, no statistically significant difference was found between group V and control,  $p = 0.135$ . On the other hand, BUN (mg/dl) was a statistically significantly lower in groups; III ( $59.51 \pm 7.96$ ), IV ( $37.69 \pm 9.5$ ) and V ( $29.15 \pm 2.78$ ) as compared to group II ( $79.86 \pm 8.81$ ),  $p = 0.001$ ,  $p < 0.0001$ , and  $p < 0.0001$ , respectively. Also, it was statistically significantly lower in group IV ( $37.69 \pm 9.5$ ) and V ( $29.15 \pm 2.78$ ) as compared to group III ( $59.51 \pm 7.96$ ),  $p = 0.001$  and  $p < 0.0001$ , respectively. Also, no statistically significant difference was found between the group IV and group V ( $p = 0.332$ ) (Figs. 38, 39).

**Serum creatinine** (mg/dl) was statistically significantly higher in group II ( $6.53 \pm 0.71$ ), III ( $5.56 \pm 0.97$ ), and IV ( $3.46 \pm 0.88$ ) as compared to control ( $1.09 \pm 0.20$ ),  $p < 0.0001$ . However, no statistically significant difference was found between group V and control,  $p = 0.053$ . On the other hand, S. creatinine (mg/dl) was a statistically significantly lower in groups; IV ( $3.46 \pm 0.88$ ) and V ( $2.40 \pm 0.42$ ) as compared to group II ( $6.53 \pm 0.71$ ),  $p < 0.0001$ . However, no statistically significant difference was found between group III and group II,  $p = 0.219$ . Also, it was statistically significantly lower in group IV ( $3.46 \pm 0.88$ ) and V ( $2.40 \pm 0.42$ ) as compared to group III ( $5.56 \pm 0.97$ ),  $p = 0.001$  and  $p < 0.0001$ , respectively. Also, no statistically significant difference was found between the group IV and group V ( $p = 0.156$ ) (Figs. 40, 41).

**TGF- $\beta$ 1** was statistically significantly higher in group II ( $13.24 \pm 1.67$ ), III ( $9.89 \pm 1.68$ ), and IV ( $6.43 \pm 1.17$ ) as compared to control ( $3.96 \pm 0.51$ ),  $p < 0.0001$ ,  $p < 0.0001$  and  $p = 0.040$ , respectively. However, no statistically significant difference was

found between group V and control,  $p = 0.931$ . On the other hand, TGF- $\beta$ 1 was a statistically significantly lower in groups; III ( $9.89 \pm 1.68$ ), and IV ( $6.43 \pm 1.17$ ) and V ( $4.58 \pm 0.83$ ) as compared to group II ( $13.24 \pm 1.67$ ),  $p < 0.0001$ ,  $p < 0.0001$ , and  $p = 0.004$ , respectively. Also, it was statistically significantly lower in group IV ( $6.43 \pm 1.17$ ) and V ( $4.58 \pm 0.83$ ) as compared to group III ( $9.89 \pm 1.68$ ),  $p = 0.003$  and  $p < 0.0001$ , respectively. Also, no statistically significant difference was found between the group IV and group V ( $p = 0.183$ ) (Figs. 42, 43).

**IL-1 $\beta$**  was statistically significantly higher in group II ( $6.23 \pm 1.08$ ), III ( $5.28 \pm 1.39$ ), and IV ( $4.49 \pm 0.64$ ) as compared to control ( $1.22 \pm 0.30$ ),  $p < 0.0001$ . However, no statistically significant difference was found between group V and control,  $p = 0.247$ . On the other hand, IL-1 $\beta$  was a statistically significantly lower in groups; IV ( $4.49 \pm 0.64$ ) and V ( $2.40 \pm 0.51$ ) as compared to group II ( $6.23 \pm 1.08$ ),  $p = 0.037$  and  $p < 0.0001$ , respectively. But the difference between group II and III was not significant,  $p = 0.454$ . Also, it was statistically significantly lower in group V ( $2.40 \pm 0.51$ ) than group III ( $5.28 \pm 1.39$ ),  $p < 0.0001$ . But the difference between group III and IV was not significant,  $p = 0.616$ . Statistically significant difference existed between the group IV and group V ( $p = 0.010$ ) (Figs. 44, 45).

**VEGF** was statistically significantly higher in group IV ( $5.34 \pm 1.29$ ), and V ( $7.92 \pm 0.99$ ) compared to control group ( $1.89 \pm 0.31$ ),  $p < 0.0001$ . However, the difference between group II and III with control was not a statistically significant,  $p = 0.178$  and  $p = 0.519$ , respectively. VEGF was a statistically significantly higher in groups; III ( $2.69 \pm 0.63$ ), IV ( $5.34 \pm 1.29$ ), and V ( $7.92 \pm 0.99$ ) as compared to group II ( $0.72 \pm 0.16$ ),  $p = 0.007$ ,  $p < 0.0001$ , and  $p < 0.0001$ , respectively. Also, it was statistically significantly higher in group IV ( $5.34 \pm 1.29$ ), and V ( $7.92 \pm 0.99$ ) when compared to group III ( $2.69 \pm 0.63$ ),  $p < 0.0001$ . Moreover, there was a statistically significant difference between the group IV and group V ( $p < 0.0001$ ) (Figs. 46, 47).

**Caspase 3** was statistically significantly higher in group II ( $4.52 \pm 0.78$ ), III ( $3.24 \pm 0.81$ ), IV ( $2.83 \pm 0.47$ ), and V ( $2.11 \pm 0.44$ ) compared to control group ( $0.72 \pm 0.15$ ),  $p < 0.0001$ ,  $p < 0.0001$ ,  $p < 0.0001$ , and  $p = 0.009$ , respectively. Caspase 3 was a statistically significantly lower in groups; III ( $3.24 \pm 0.81$ ), IV ( $2.83 \pm 0.47$ ), and V ( $2.11 \pm 0.44$ ) as compared to group II ( $4.52 \pm 0.78$ ),  $p = 0.019$ ,  $p = 0.002$ , and  $p < 0.0001$ , respectively. Also, it was statistically significantly lower in group V ( $2.11 \pm 0.44$ ) than group III ( $3.24 \pm 0.81$ ),  $p = 0.042$ . However, the difference between group III and IV was not a statistically significant,  $p = 0.793$ . Likewise, no

statistically significant difference was found between the group IV and group V ( $p=0.323$ ) (**Figs. 48.49**).

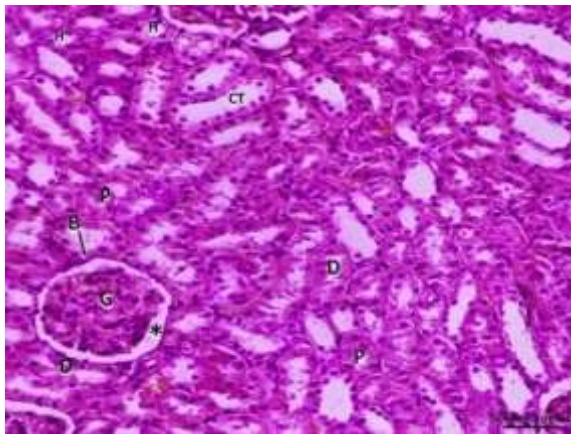


**Fig.1:** A photomicrograph of a cross section of the renal cortex and medulla of group I (Normal control) showing Proximal (P), distal (D) convoluted tubules, renal corpuscles; formed of a dense rounded glomerulus (G) surrounded by a parietal layer of Bowman's capsule (B) with the urinary space (\*) in-between. Collecting tubules (CT) and loops of Henle (H) can be observed in the renal medulla. (Hx. & E.X200)

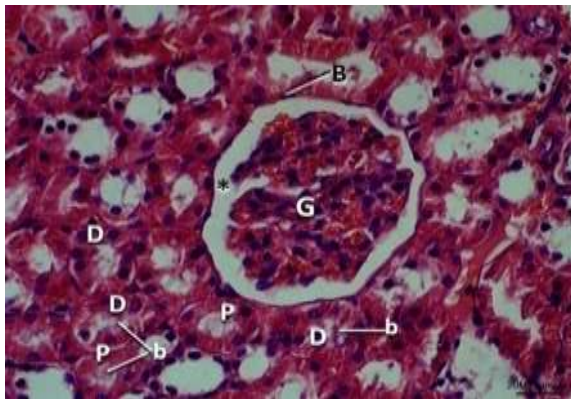


**Fig.2:** A photomicrograph of a cross section of the renal cortex of group I showing renal corpuscles, formed of a dense rounded glomerulus (G) surrounded by a parietal layer of Bowman's capsule (B) with the urinary space (\*) in-between. Proximal convoluted tubules (P) are lined with low columnar cells with strongly acidophilic cytoplasm and spherical basal nuclei. The distal convoluted tubules (D) are lined with low cuboidal cells with faint acidophilic cytoplasm and rounded central nuclei. An intact apical brush border (b) of proximal and distal convoluted tubule can be observed. (Hx. & E.X400)

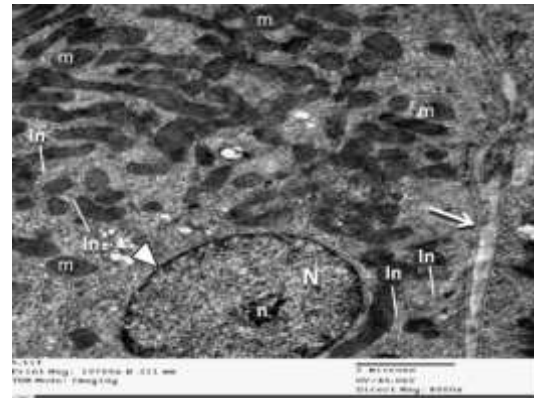


**Fig.3:** An electron micrograph of group I displaying a proximal convoluted tubular cell with heterochromatic nucleus (N) with prominent nucleolus (n) and intact nuclear envelop (arrowhead), abundant parallel electron dense mitochondria (m) are situated between the nucleus and a uniformly thin basal cell membrane (thin arrow) and intact basal infoldings (In) (EM X 8000).

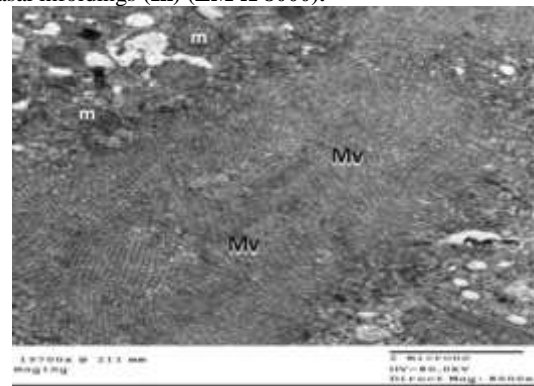


**Fig.4:** An electron micrograph of group I displaying a proximal convoluted tubular cell with electron dense mitochondria (m) and intact apical microvilli (Mv) (EM X 8000).

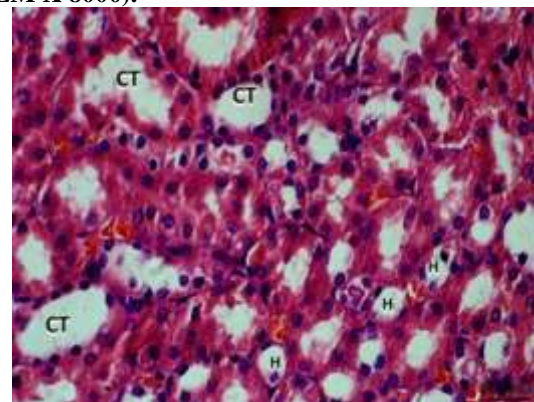


**Fig. 5:** A photomicrograph of a cross section of the renal medulla of group I featuring collecting tubules (CT) lined with simple columnar epithelium and loops of Henle (H) lined with simple cuboidal epithelium with scanty cytoplasm and bulging nuclei into the lumen. (Hx. & E.X400)

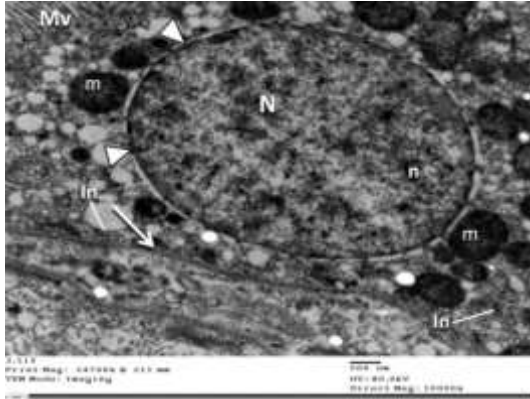


**Fig. 6:** An electron micrograph of group I displaying an epithelial lining cell of medullary thick ascending limb of Henle with heterochromatic nucleus (N) with prominent nucleolus (n) and intact nuclear envelop (arrowhead), basal infoldings (In), a uniformly thin basal cell membrane (thin arrow) and abundant electron dense mitochondria (m) with intact cristae (EM x 10000).

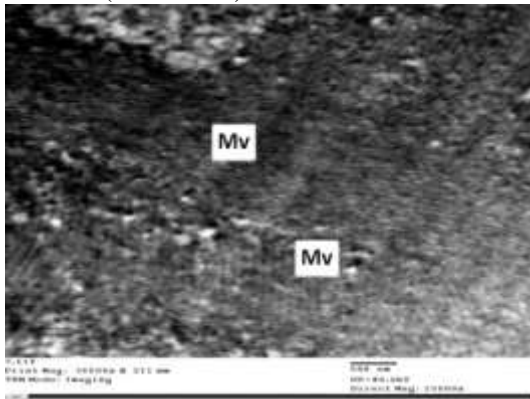


**Fig. 7:** An electron micrograph of group I displaying an epithelial lining cell of medullary thick ascending limb of Henle with intact apical microvilli (Mv) (EM x 15000)

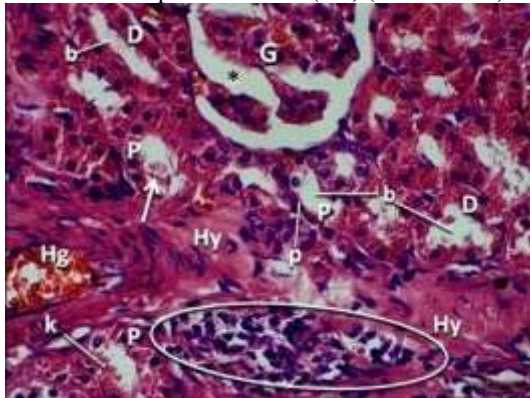


**Fig.8:** A photomicrograph of a cross section of the renal cortex of group II (Cyclosporine A administration) showing extremely shrunken glomeruli (G) with a widened urinary space (\*) in-between. Most of proximal (P) and distal (D) convoluted tubules exhibit lost apical brush border (b), intraluminal casts (arrow), with pyknotic (p), karyolytic (k) nuclei. The interstitial tissue features areas of hyaline (Hy) degeneration, haemorrhage (Hg) and mononuclear cell infiltration (circle). (Hx. & E.X 400)

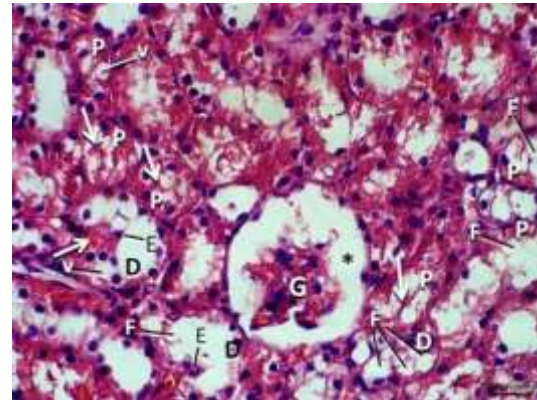


**Fig.9:** A photomicrograph of a cross section of the renal cortex of group II showing extremely shrunken glomeruli (G) with a widened urinary space (\*) in-between. Most of proximal (P) and distal (D) convoluted tubules exhibit extensive fat degeneration (F), cytoplasmic vacuolation (v), intra-luminal casts (arrow) and exfoliation (E) of lining epithelial cells (Hx. & E.X 400)

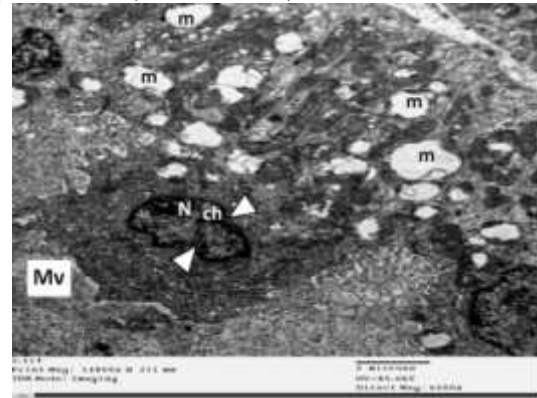


**Fig.10:** An electron micrograph of group II displaying a proximal convoluted tubular cell with extremely shrunken nucleus (N) with clumped chromatin (ch) and intended nuclear envelope (arrowhead), ballooned mitochondria (m) with damaged cristae and lost apical microvilli (Mv) (EM X6000).

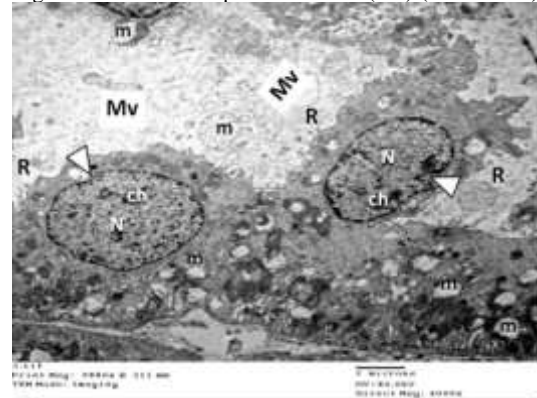


**Fig.11:** An electron micrograph of group II displaying proximal convoluted tubular cells with karyolytic nuclei (N) with clumped chromatin (ch) and intended nuclear envelope (arrowhead), extensive cytoplasmic rarefaction (R) ballooned mitochondria (m) with damaged cristae and lost apical microvilli (Mv) (EM X6000).

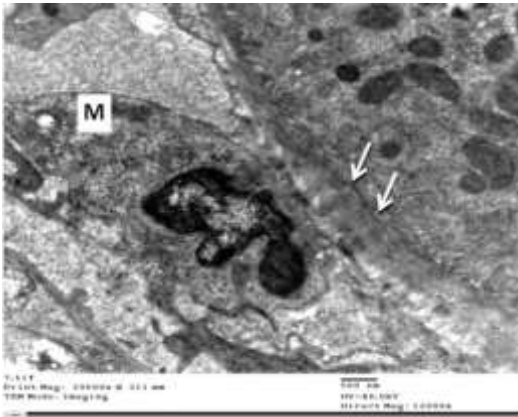


**Fig.12:** An electron micrograph of group II displaying proximal convoluted tubular cells with extremely thickened basal cell membrane (thin arrow) and absent basal infoldings. A macrophage (M) can be observed in the interstitial tissue (EM X12000).

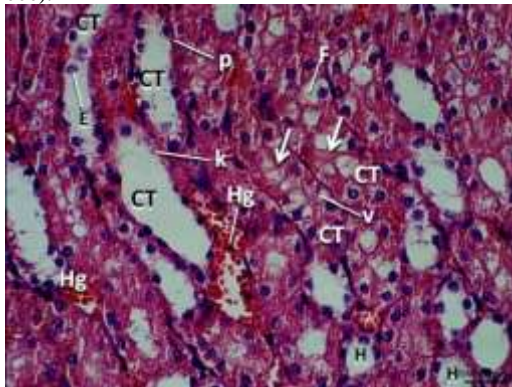


**Fig.13:** A photomicrograph of a cross section of the renal medulla of group II showing loops of Henle (H) and collecting tubules (CT) with intra-luminal casts (arrow), nuclear pyknosis (p), karyolysis (k), exfoliation (E) of lining epithelial cells, cytoplasmic vacuolation (v) and fat degeneration (F). The interstitial tissue features areas of haemorrhage (Hg) (Hx. & E.X 400)

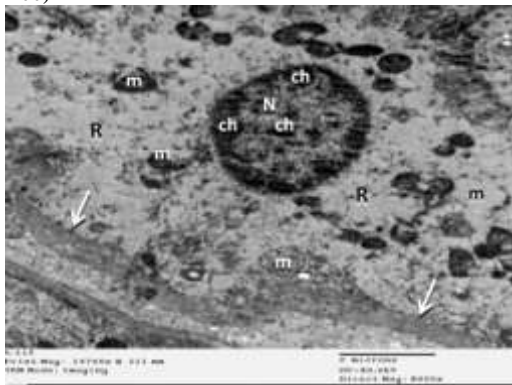


**Fig. 14:** An electron micrograph of group II displaying an epithelial lining cell of medullary thick ascending limb of Henle with a degenerated nucleus (N) with clumped chromatin (ch), extensive cytoplasmic rarefaction (R) ballooned mitochondria (m) with damaged cristae and extremely thickened basal cell membrane (thin arrow) (EM X8000).

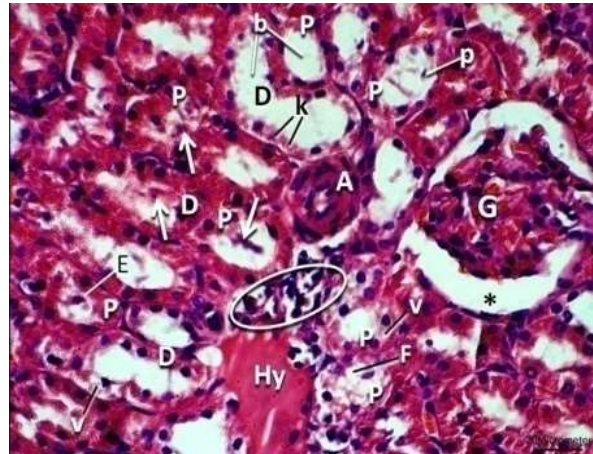


**Fig.15:** A photomicrograph of a cross section of the renal cortex of group III (Cyclosporine A administration with spontaneous recovery): showing extremely shrunken glomeruli (G) with a widened urinary space (\*) in-between. Most of proximal (P) and distal (D) convoluted tubules exhibit lost apical brush border (b), intra-luminal casts (arrow), exfoliation (E) of lining epithelial cells, cytoplasmic vacuolation (v), fat degeneration (F) with pyknotic (p), karyotic (k) nuclei. The interstitial tissue features few areas of hyaline (Hy) degeneration. (Hx. & E.X 400)

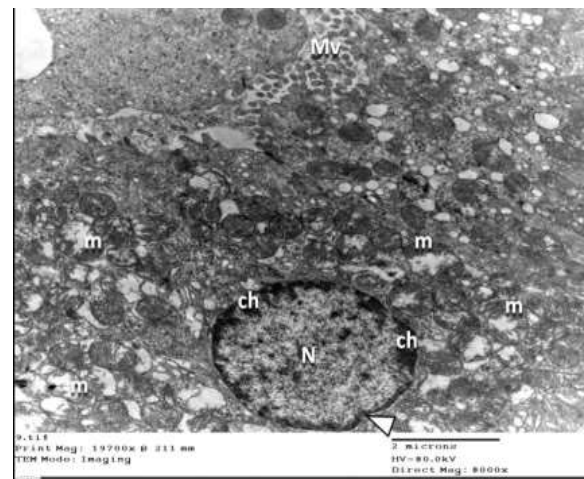


**Fig.16:** An electron micrograph of group III displaying proximal convoluted tubular cells with a degenerated nucleus (N) with clumped chromatin (ch) and indented nuclear envelope (arrowhead), pathological aggregation of ballooned mitochondria (m) with damaged cristae and partially damaged microvilli (Mv) (EM X8000).

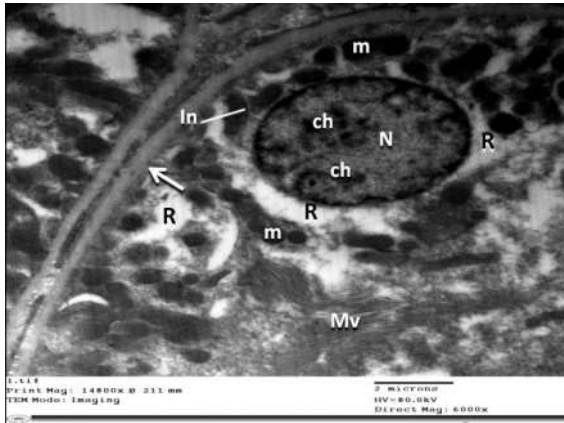


**Fig.17:** An electron micrograph of group III displaying proximal convoluted tubular cells with a degenerated nucleus (N) with clumped chromatin (ch), mild cytoplasmic rarefaction (R), moderately thickened basal cell membrane (thin arrow) with intact basal infoldings (In), abundant mitochondria (m) with intact cristae and intact apical microvilli (Mv) (EM X8000).

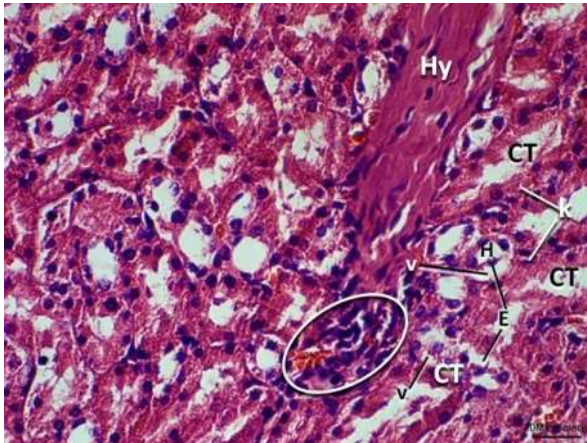


**Fig.18:** A photomicrograph of a cross section of the renal medulla of group III showing loops of Henle (H) and collecting tubules (CT) with cytoplasmic vacuolation (v), karyolitic nuclei (k) and exfoliation (E) of lining epithelial cells. The interstitial tissue features areas of hyaline (Hy) degeneration, and mononuclear cell infiltration (circle). (Hx. & E.X 400)

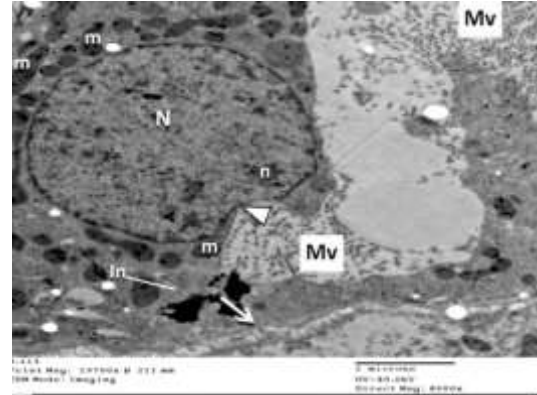


**Fig. 19:** An electron micrograph of group III displaying an epithelial lining cell of medullary thick ascending limb of Henle with a karyolytic nucleus (N) with indented nuclear envelope (arrowhead) intact mitochondria (m) with intact cristae, partially damaged apical microvilli (Mv) and thin basal cell membrane (thin arrow) with intact basal infoldings (In) (EM X8000).

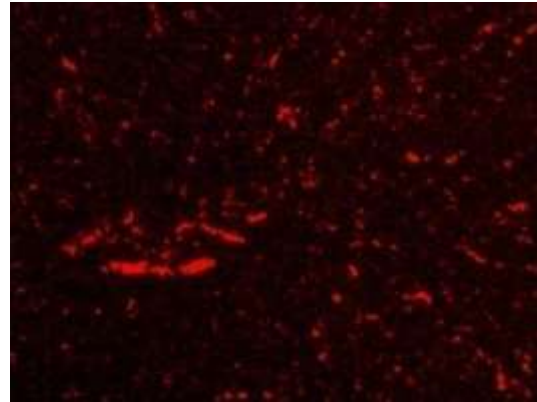


**Fig.20:** Labelling of MSCs with PKH26 dye in group IV (Cyclosporine A and stem cells administration):

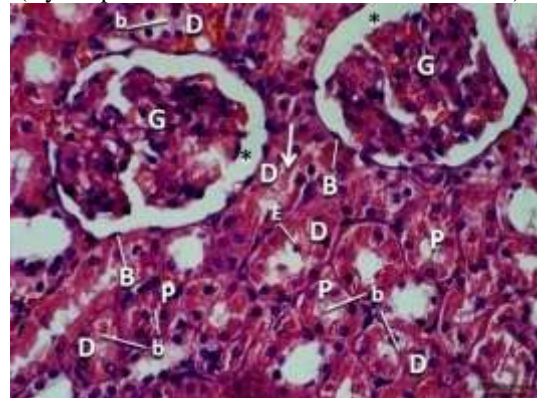


**Fig.21:** A photomicrograph of a cross section of the renal cortex of group IV showing almost normal glomeruli (G) surrounded by a parietal layer of Bowman's capsule (B) with the urinary space (\*) in-between. Some proximal (P) and distal (D) convoluted tubules exhibit intact apical brush border (b) but few of them display intra-luminal casts (arrow) and exfoliation (E) of lining epithelial cells, (Hx. & E.X 400)

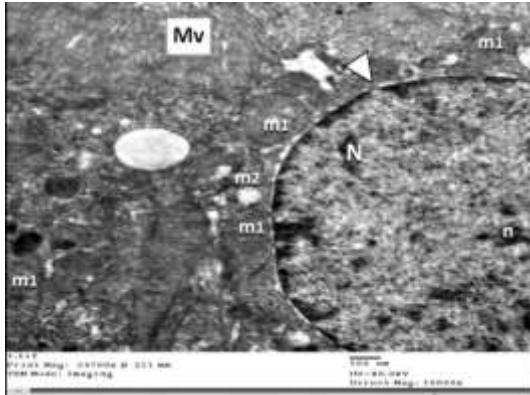


**Fig.22:** An electron micrograph of group IV displaying a proximal convoluted tubular cell with a heterochromatic nucleus (N) with prominent nucleolus (n) and intact nuclear envelop (arrowhead), intact apical microvilli (Mv) and abundant intact mitochondria (m<sup>1</sup>) with intact cristae but few of them are ballooned with damaged cristae (m<sup>2</sup>).

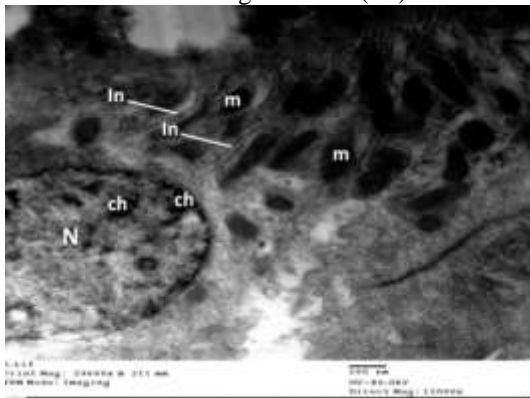


**Fig.23:** An electron micrograph of group IV displaying a proximal convoluted tubular cell with a degenerated nucleus with clumped chromatin (ch), intact mitochondria (m) with intact cristae and intact basal infoldings (In) (EM X 12000).

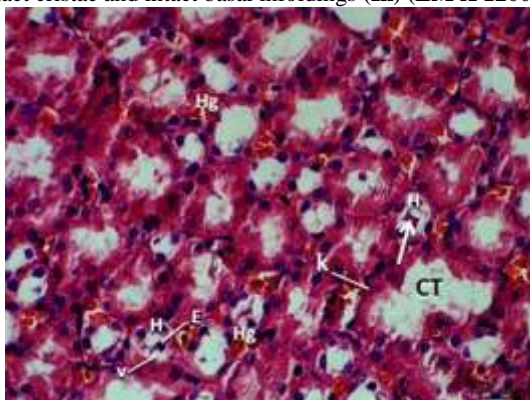


**Fig.24:** A photomicrograph of a cross section of the renal medulla of group IV showing some loops of Henle (H) and collecting tubules (CT) with cytoplasmic vacuolation (v), karyolytic nuclei (k), intra-luminal casts (arrow) and exfoliation (E) of lining epithelial cells. The interstitial tissue features few areas of haemorrhage (Hg). (Hx. & E.X 400)

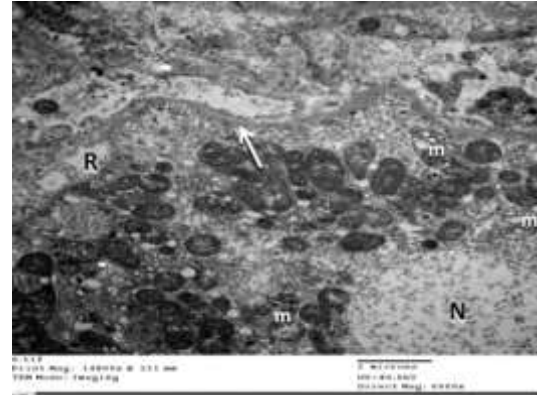


**Fig. 25:** An electron micrograph of group IV displaying an epithelial lining cell of medullary thick ascending limb of Henle with an extremely karyolytic nucleus (N), mild cytoplasmic rarefaction (R), ballooned mitochondria (m) with damaged cristae, mildly thickened basal cell membrane (thin arrow) (EM X6000).

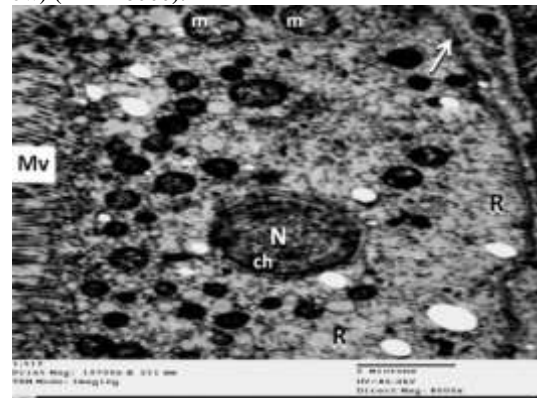


**Fig. 26:** An electron micrograph of group IV displaying an epithelial lining cell of medullary thick ascending limb of Henle with degenerated nucleus (N) with clumped chromatin (ch) ballooned mitochondria (m) with damaged cristae, intact apical microvilli (Mv) and thin basal cell membrane (thin arrow) with lost basal infoldings (EM X8000).

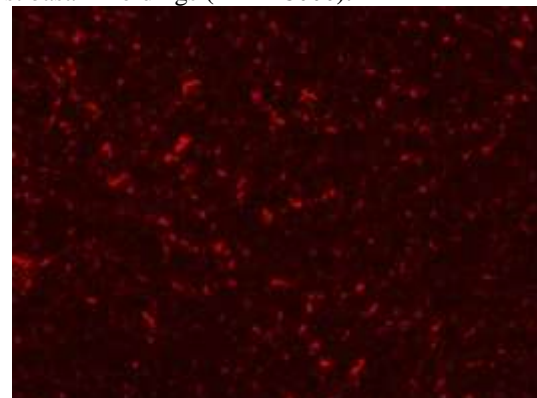


**Fig.27:** Labelling of MSCs with PKH26 dye in group V (Cyclosporine A, stem cells with erythropoietin pre-administration):

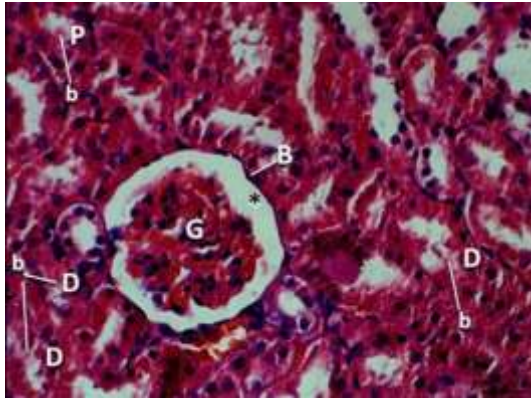


**Fig.28:** A photomicrograph of a cross section of the renal cortex of group V showing apparently normal renal corpuscles, formed of a dense rounded glomerulus (G) surrounded by a parietal layer of Bowman's capsule (B) with the urinary space (\*) in-between. Proximal convoluted tubules (P) and distal convoluted tubules (D) with intact apical brush border (b). (Hx. & E.X400)

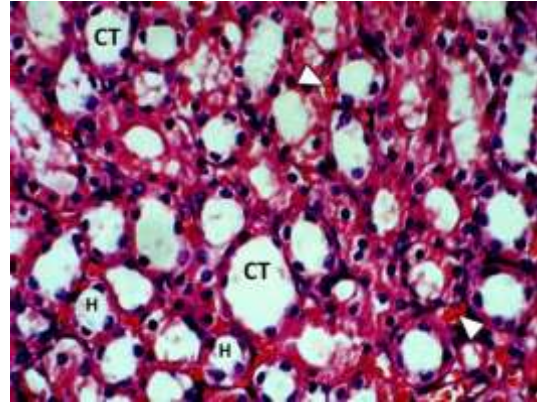


**Fig.30:** A photomicrograph of a cross section of the renal medulla of group V showing apparently normal loops of Henle (H) and collecting tubules (CT) with mildly congested blood vessels (arrowhead) in-between (Hx. & E.X 400).

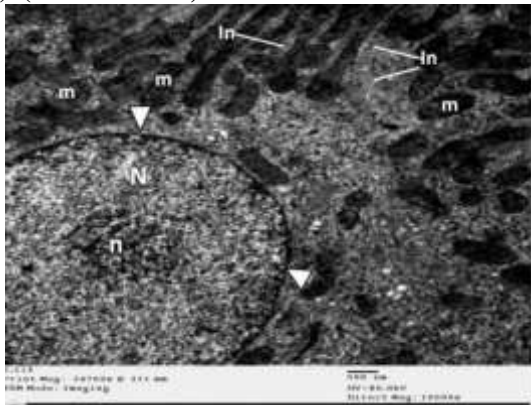


**Fig.29:** An electron micrograph of group V displaying an apparently normal proximal convoluted tubular cell with heterochromatic nucleus (N) with prominent nucleolus (n) and intact nuclear envelop (arrowhead), abundant parallel electron dense mitochondria (m) and intact basal infoldings (In) (EM X 10000).

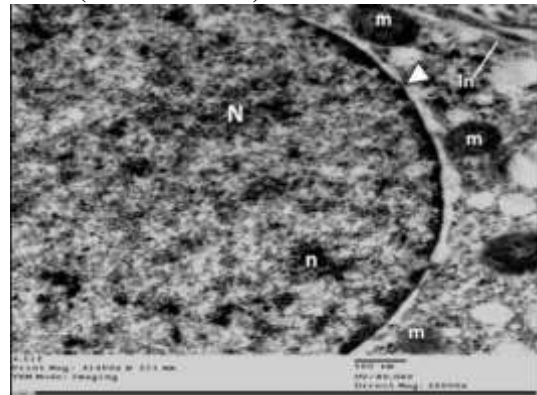
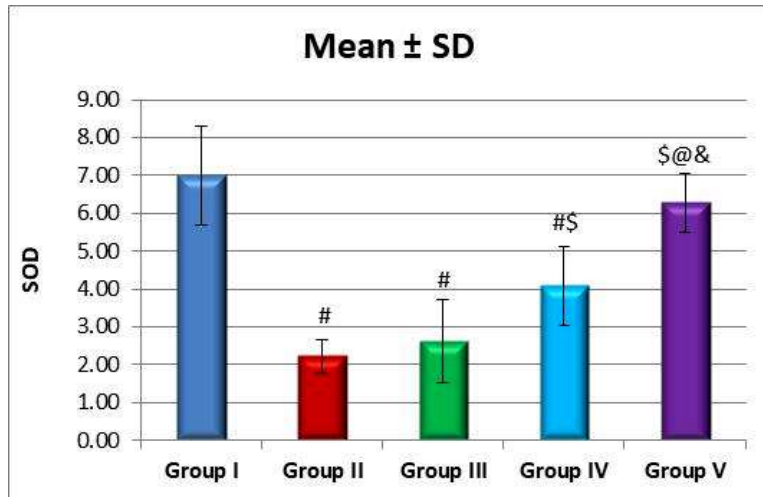


**Fig. 31:** An electron micrograph of group V displaying an apparently normal epithelial lining cell of medullary thick ascending limb of Henle with heterochromatic nucleus (N) with prominent nucleolus (n) and intact nuclear envelop (arrowhead), intact basal infoldings (In) and abundant electron dense mitochondria (m) with intact cristae (EM x 20000).

**Fig. 32:** A table illustrating mean values of SOD in rat kidney specimens obtained from different groups of the examined animals.

|                 | Group I (Control) |      | Group II |      | Group III |      | Group IV |      | Group V |      |
|-----------------|-------------------|------|----------|------|-----------|------|----------|------|---------|------|
|                 | Mean              | SD   | Mean     | SD   | Mean      | SD   | Mean     | SD   | Mean    | SD   |
| <b>SOD</b>      | 6.99              | 1.29 | 2.23     | 0.42 | 2.62      | 1.11 | 4.08     | 1.03 | 6.29    | 0.77 |
| <b>P-values</b> |                   |      |          |      |           |      |          |      |         |      |
| G I vs. G II    | <0.0001 (S)       |      |          |      |           |      |          |      |         |      |
| G I vs. G III   | <0.0001 (S)       |      |          |      |           |      |          |      |         |      |
| G I vs. G IV    | <0.0001 (S)       |      |          |      |           |      |          |      |         |      |
| G I vs. G V     | 0.780 (NS)        |      |          |      |           |      |          |      |         |      |
| G II vs. G III  | 0.966 (NS)        |      |          |      |           |      |          |      |         |      |
| G II vs. G IV   | 0.048 (S)         |      |          |      |           |      |          |      |         |      |
| G II vs. G V    | <0.0001 (S)       |      |          |      |           |      |          |      |         |      |
| G III vs. G IV  | 0.166 (NS)        |      |          |      |           |      |          |      |         |      |
| G III vs. G V   | <0.0001 (S)       |      |          |      |           |      |          |      |         |      |
| G IV vs. G V    | 0.014 (S)         |      |          |      |           |      |          |      |         |      |

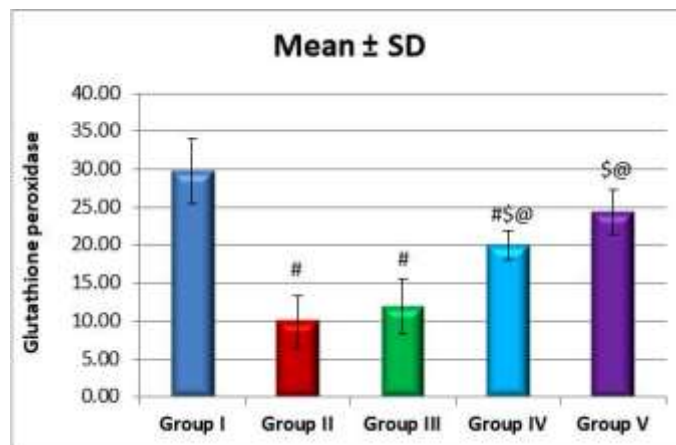


# significant from control, \$ significant from group II, @ significant from group III & significant from group IV

**Fig.33:** A **Histogram:** illustrating mean values of SOD in rat kidney specimens obtained from different groups of the examined animals.

**Fig. 34:** A table illustrating mean values of Glutathione peroxidase in rat kidney specimens obtained from different groups of the examined animals

|                               | Group I (Control) |      | Group II    |      | Group III   |      | Group IV   |      | Group V |      |
|-------------------------------|-------------------|------|-------------|------|-------------|------|------------|------|---------|------|
|                               | Mean              | SD   | Mean        | SD   | Mean        | SD   | Mean       | SD   | Mean    | SD   |
| <b>Glutathione peroxidase</b> | 29.76             | 4.33 | 10.01       | 3.39 | 11.87       | 3.61 | 20.05      | 1.95 | 24.30   | 2.95 |
| <b>P-values</b>               |                   |      |             |      |             |      |            |      |         |      |
| G I vs. G II                  | <0.0001 (S)       |      |             |      |             |      |            |      |         |      |
| G I vs. G III                 | <0.0001 (S)       |      |             |      |             |      |            |      |         |      |
| G I vs. G IV                  | 0.001 (S)         |      |             |      |             |      |            |      |         |      |
| G I vs. G V                   | 0.112 (NS)        |      |             |      |             |      |            |      |         |      |
| G II vs. G III                |                   |      | 0.900 (NS)  |      |             |      |            |      |         |      |
| G II vs. G IV                 |                   |      | 0.001 (S)   |      |             |      |            |      |         |      |
| G II vs. G V                  |                   |      | <0.0001 (S) |      |             |      |            |      |         |      |
| G III vs. G IV                |                   |      |             |      | 0.008 (S)   |      |            |      |         |      |
| G III vs. G V                 |                   |      |             |      | <0.0001 (S) |      |            |      |         |      |
| G IV vs. G V                  |                   |      |             |      |             |      | 0.294 (NS) |      |         |      |

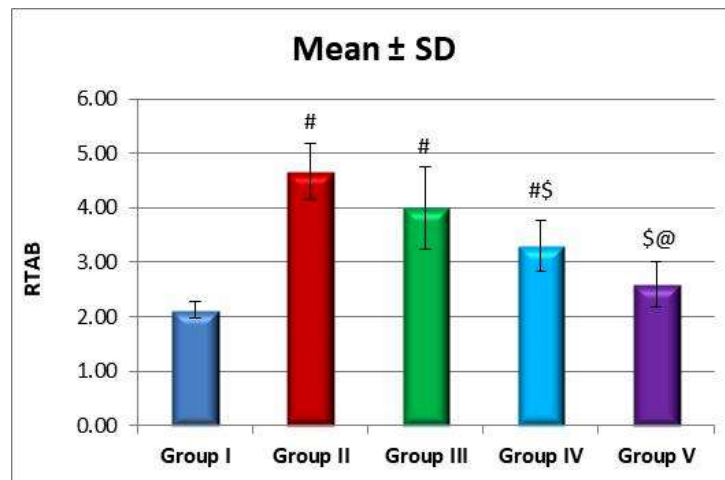


# significant from control,\$ significant from group II,@ significant from group III & significant from group IV

**Fig. 35:** A **Histogram:** illustrating mean values of Glutathione peroxidase in rat kidney specimens obtained from different groups of the examined animals.

**Fig 36:** A table illustrating mean values of RTBA in rat kidney specimens obtained from different groups of the examined animals.

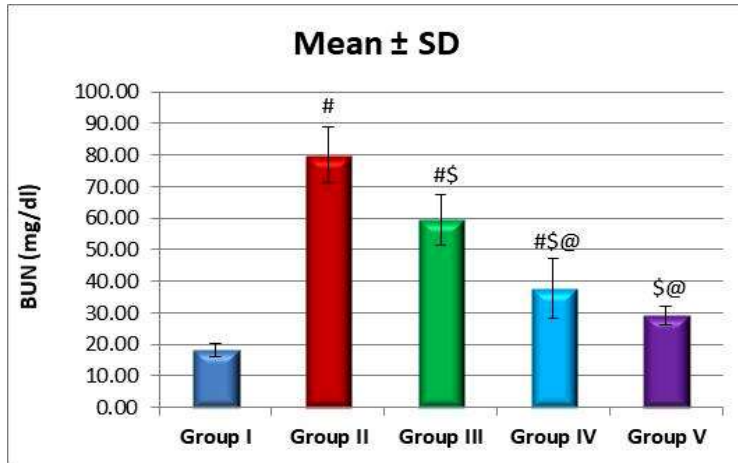
|                 | Group I (Control) |      | Group II    |      | Group III  |      | Group IV   |      | Group V |      |
|-----------------|-------------------|------|-------------|------|------------|------|------------|------|---------|------|
|                 | Mean              | SD   | Mean        | SD   | Mean       | SD   | Mean       | SD   | Mean    | SD   |
| <b>RTBA</b>     | 2.12              | 0.15 | 4.66        | 0.52 | 3.99       | 0.76 | 3.30       | 0.47 | 2.59    | 0.42 |
| <b>P-values</b> |                   |      |             |      |            |      |            |      |         |      |
| G I vs. G II    | <0.0001 (S)       |      |             |      |            |      |            |      |         |      |
| G I vs. G III   | <0.0001 (S)       |      |             |      |            |      |            |      |         |      |
| G I vs. G IV    | 0.041 (S)         |      |             |      |            |      |            |      |         |      |
| G I vs. G V     | 0.588 (NS)        |      |             |      |            |      |            |      |         |      |
| G II vs. G III  |                   |      | 0.255 (NS)  |      |            |      |            |      |         |      |
| G II vs. G IV   |                   |      | 0.003 (S)   |      |            |      |            |      |         |      |
| G II vs. G V    |                   |      | <0.0001 (S) |      |            |      |            |      |         |      |
| G III vs. G IV  |                   |      |             |      | 0.233 (NS) |      |            |      |         |      |
| G III vs. G V   |                   |      |             |      | 0.002 (S)  |      |            |      |         |      |
| G IV vs. G V    |                   |      |             |      |            |      | 0.219 (NS) |      |         |      |



# significant from control, \$ significant from group II, @ significant from group III & significant from group IV

**Fig. 37:** A Histogram: illustrating mean values of RTBA in rat kidney specimens obtained from different groups of the examined animals.**Fig. 38:** A table illustrating mean values of BUN obtained from different groups of the examined animals.

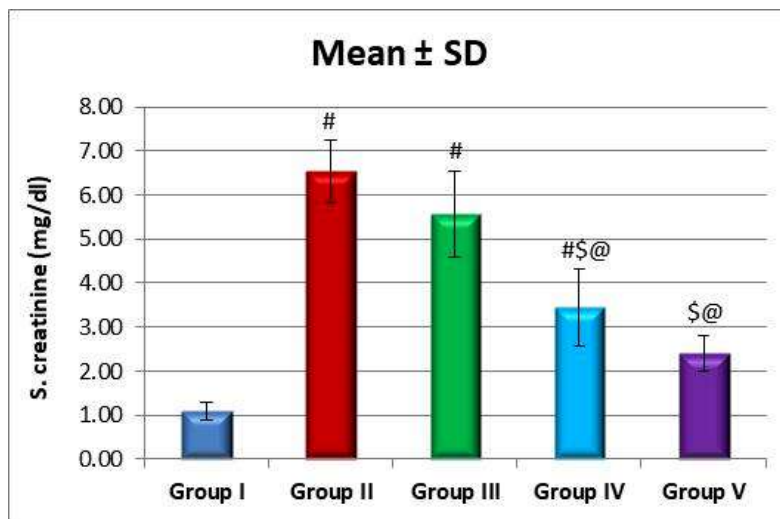
|                 | Group I (Control) |      | Group II    |      | Group III   |      | Group IV   |      | Group V |      |
|-----------------|-------------------|------|-------------|------|-------------|------|------------|------|---------|------|
|                 | Mean              | SD   | Mean        | SD   | Mean        | SD   | Mean       | SD   | Mean    | SD   |
| <b>BUN</b>      | 18.20             | 2.14 | 79.86       | 8.81 | 59.51       | 7.96 | 37.69      | 9.50 | 29.15   | 2.78 |
| <b>P-values</b> |                   |      |             |      |             |      |            |      |         |      |
| G I vs. G II    | <0.0001 (S)       |      |             |      |             |      |            |      |         |      |
| G I vs. G III   | <0.0001 (S)       |      |             |      |             |      |            |      |         |      |
| G I vs. G IV    | 0.002 (S)         |      |             |      |             |      |            |      |         |      |
| G I vs. G V     | 0.135 (NS)        |      |             |      |             |      |            |      |         |      |
| G II vs. G III  |                   |      | 0.001 (S)   |      |             |      |            |      |         |      |
| G II vs. G IV   |                   |      | <0.0001 (S) |      |             |      |            |      |         |      |
| G II vs. G V    |                   |      | <0.0001 (S) |      |             |      |            |      |         |      |
| G III vs. G IV  |                   |      |             |      | 0.001 (S)   |      |            |      |         |      |
| G III vs. G V   |                   |      |             |      | <0.0001 (S) |      |            |      |         |      |
| G IV vs. G V    |                   |      |             |      |             |      | 0.332 (NS) |      |         |      |



# significant from control, \$ significant from group II, @ significant from group III & significant from group IV  
**Fig. 39:** A Histogram: illustrating mean values of BUN obtained from different groups of the examined animals.

**Fig. 40:** A table illustrating mean values of serum creatinine obtained from different groups of the examined animals.

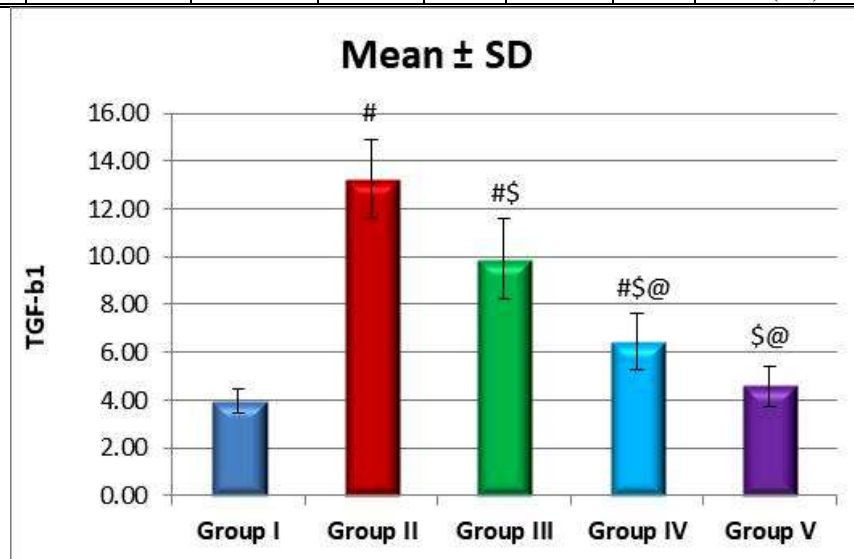
|                      | Group I (Control) |      | Group II    |      | Group III   |      | Group IV   |      | Group V |      |
|----------------------|-------------------|------|-------------|------|-------------|------|------------|------|---------|------|
|                      | Mean              | SD   | Mean        | SD   | Mean        | SD   | Mean       | SD   | Mean    | SD   |
| <b>S. creatinine</b> | 1.09              | 0.20 | 6.53        | 0.71 | 5.56        | 0.97 | 3.46       | 0.88 | 2.40    | 0.42 |
| <b>P-values</b>      |                   |      |             |      |             |      |            |      |         |      |
| G I vs. G II         | <0.0001 (S)       |      |             |      |             |      |            |      |         |      |
| G I vs. G III        | <0.0001 (S)       |      |             |      |             |      |            |      |         |      |
| G I vs. G IV         | <0.0001 (S)       |      |             |      |             |      |            |      |         |      |
| G I vs. G V          | 0.053 (NS)        |      |             |      |             |      |            |      |         |      |
| G II vs. G III       |                   |      | 0.219 (NS)  |      |             |      |            |      |         |      |
| G II vs. G IV        |                   |      | <0.0001 (S) |      |             |      |            |      |         |      |
| G II vs. G V         |                   |      | <0.0001 (S) |      |             |      |            |      |         |      |
| G III vs. G IV       |                   |      |             |      | 0.001 (S)   |      |            |      |         |      |
| G III vs. G V        |                   |      |             |      | <0.0001 (S) |      |            |      |         |      |
| G IV vs. G V         |                   |      |             |      |             |      | 0.156 (NS) |      |         |      |



# significant from control, \$ significant from group II, @ significant from group III & significant from group IV  
**Fig. 41:** A Histogram: illustrating mean values of serum creatinine obtained from different groups of the examined animals.

**Fig. 42:** A table illustrating mean values of TGF-b1 obtained from different groups of the examined animals.

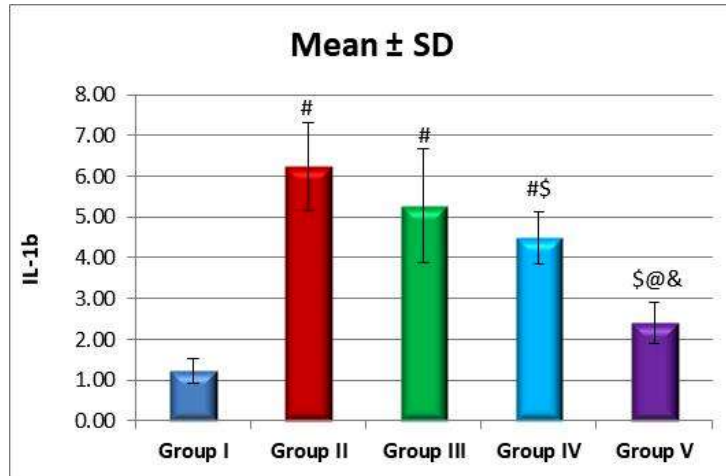
|                 | Group I (Control) |      | Group II |      | Group III |      | Group IV |      | Group V |      |
|-----------------|-------------------|------|----------|------|-----------|------|----------|------|---------|------|
|                 | Mean              | SD   | Mean     | SD   | Mean      | SD   | Mean     | SD   | Mean    | SD   |
| <b>TGF-b1</b>   | 3.96              | 0.51 | 13.24    | 1.67 | 9.89      | 1.68 | 6.43     | 1.17 | 4.58    | 0.83 |
| <b>P-values</b> |                   |      |          |      |           |      |          |      |         |      |
| G I vs. G II    | <0.0001 (S)       |      |          |      |           |      |          |      |         |      |
| G I vs. G III   | <0.0001 (S)       |      |          |      |           |      |          |      |         |      |
| G I vs. G IV    | 0.040 (S)         |      |          |      |           |      |          |      |         |      |
| G I vs. G V     | 0.931 (NS)        |      |          |      |           |      |          |      |         |      |
| G II vs. G III  | 0.004 (S)         |      |          |      |           |      |          |      |         |      |
| G II vs. G IV   | <0.0001 (S)       |      |          |      |           |      |          |      |         |      |
| G II vs. G V    | <0.0001 (S)       |      |          |      |           |      |          |      |         |      |
| G III vs. G IV  | 0.003 (S)         |      |          |      |           |      |          |      |         |      |
| G III vs. G V   | <0.0001 (S)       |      |          |      |           |      |          |      |         |      |
| G IV vs. G V    | 0.183 (NS)        |      |          |      |           |      |          |      |         |      |



# significant from control, \$ significant from group II, @ significant from group III & significant from group IV

**Fig. 43:** A Histogram: illustrating mean values of TGF-b1 obtained from different groups of the examined animals.**Fig. 44:** A table illustrating mean values of IL-1b obtained from different groups of the examined animals

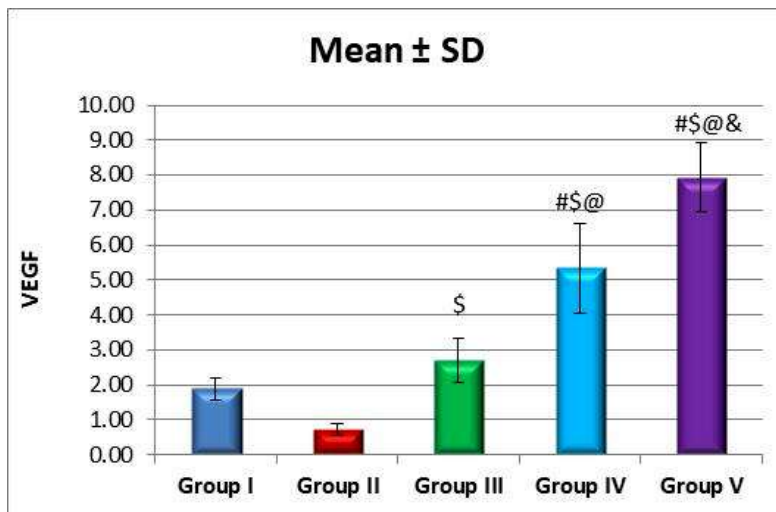
|                 | Group I (Control) |      | Group II |      | Group III |      | Group IV |      | Group V |      |
|-----------------|-------------------|------|----------|------|-----------|------|----------|------|---------|------|
|                 | Mean              | SD   | Mean     | SD   | Mean      | SD   | Mean     | SD   | Mean    | SD   |
| <b>IL-1b</b>    | 1.22              | 0.30 | 6.23     | 1.08 | 5.28      | 1.39 | 4.49     | 0.64 | 2.40    | 0.51 |
| <b>P-values</b> |                   |      |          |      |           |      |          |      |         |      |
| G I vs. G II    | <0.0001 (S)       |      |          |      |           |      |          |      |         |      |
| G I vs. G III   | <0.0001 (S)       |      |          |      |           |      |          |      |         |      |
| G I vs. G IV    | <0.0001 (S)       |      |          |      |           |      |          |      |         |      |
| G I vs. G V     | 0.247 (NS)        |      |          |      |           |      |          |      |         |      |
| G II vs. G III  | 0.454 (NS)        |      |          |      |           |      |          |      |         |      |
| G II vs. G IV   | 0.037 (S)         |      |          |      |           |      |          |      |         |      |
| G II vs. G V    | <0.0001 (S)       |      |          |      |           |      |          |      |         |      |
| G III vs. G IV  | 0.616 (NS)        |      |          |      |           |      |          |      |         |      |
| G III vs. G V   | <0.0001 (S)       |      |          |      |           |      |          |      |         |      |
| G IV vs. G V    | 0.010 (S)         |      |          |      |           |      |          |      |         |      |



# significant from control, \$ significant from group II, @ significant from group III & significant from group IV  
**Fig. 45:** A Histogram: illustrating mean values of IL-1b obtained from different groups of the examined animals.

**Fig. 46:** A table illustrating mean values of VEGF obtained from different groups of the examined animals.

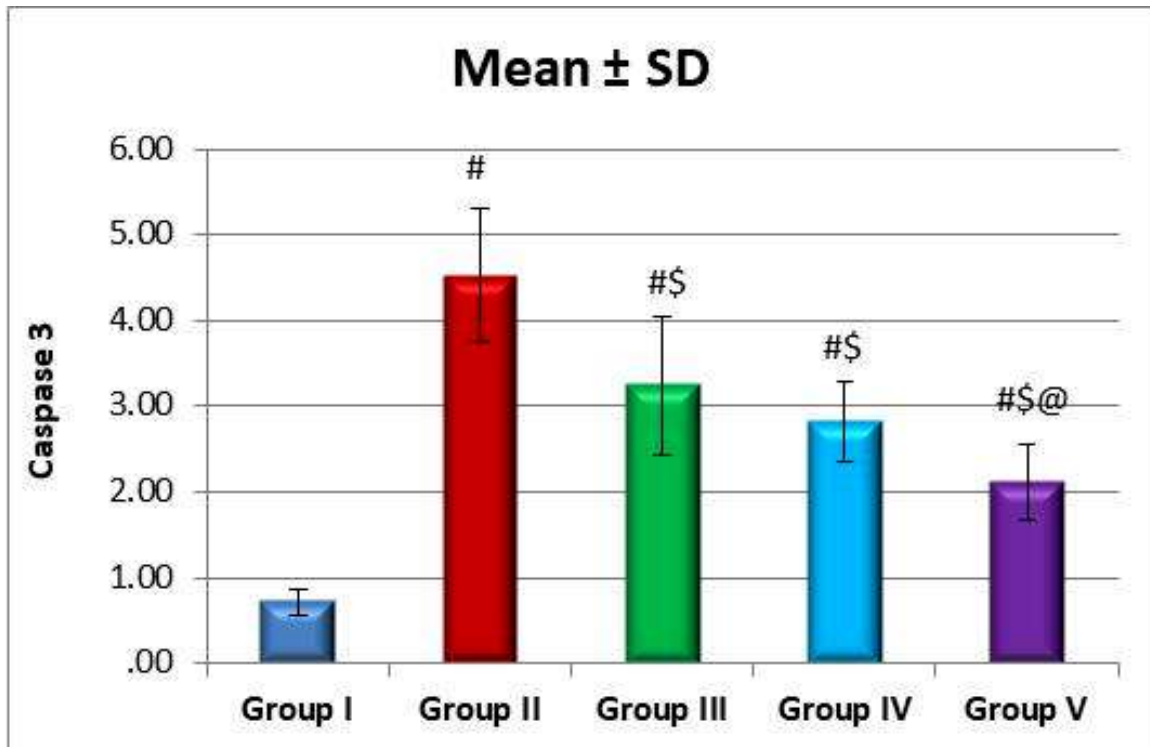
|                 | Group I (Control) |      | Group II |      | Group III |      | Group IV |      | Group V |      |
|-----------------|-------------------|------|----------|------|-----------|------|----------|------|---------|------|
|                 | Mean              | SD   | Mean     | SD   | Mean      | SD   | Mean     | SD   | Mean    | SD   |
| <b>VEGF</b>     | 1.89              | 0.31 | 0.72     | 0.16 | 2.69      | 0.63 | 5.34     | 1.29 | 7.92    | 0.99 |
| <b>P-values</b> |                   |      |          |      |           |      |          |      |         |      |
| G I vs. G II    | 0.178(NS)         |      |          |      |           |      |          |      |         |      |
| G I vs. G III   | 0.519 (NS)        |      |          |      |           |      |          |      |         |      |
| G I vs. G IV    | <0.0001 (S)       |      |          |      |           |      |          |      |         |      |
| G I vs. G V     | <0.0001 (S)       |      |          |      |           |      |          |      |         |      |
| G II vs. G III  | 0.007 (S)         |      |          |      |           |      |          |      |         |      |
| G II vs. G IV   | <0.0001 (S)       |      |          |      |           |      |          |      |         |      |
| G II vs. G V    | <0.0001 (S)       |      |          |      |           |      |          |      |         |      |
| G III vs. G IV  | <0.0001 (S)       |      |          |      |           |      |          |      |         |      |
| G III vs. G V   | <0.0001 (S)       |      |          |      |           |      |          |      |         |      |
| G IV vs. G V    | <0.0001 (S)       |      |          |      |           |      |          |      |         |      |



# significant from control, \$ significant from group II, @ significant from group III & significant from group IV  
**Fig. 47:** A Histogram: illustrating mean values of VEGF obtained from different groups of the examined animals.

**Fig. 48:** A table illustrating mean values of Caspase 3 obtained from different groups of the examined animals.

|                  | Group I (Control) |      | Group II    |      | Group III  |      | Group IV   |      | Group V |      |
|------------------|-------------------|------|-------------|------|------------|------|------------|------|---------|------|
|                  | Mean              | SD   | Mean        | SD   | Mean       | SD   | Mean       | SD   | Mean    | SD   |
| <b>Caspase 3</b> | 0.72              | 0.15 | 4.52        | 0.78 | 3.24       | 0.81 | 2.83       | 0.47 | 2.11    | 0.44 |
| <b>P-values</b>  |                   |      |             |      |            |      |            |      |         |      |
| G I vs. G II     | <0.0001 (S)       |      |             |      |            |      |            |      |         |      |
| G I vs. G III    | <0.0001 (S)       |      |             |      |            |      |            |      |         |      |
| G I vs. G IV     | <0.0001 (S)       |      |             |      |            |      |            |      |         |      |
| G I vs. G V      | 0.009 (S)         |      |             |      |            |      |            |      |         |      |
| G II vs. G III   |                   |      | 0.019 (S)   |      |            |      |            |      |         |      |
| G II vs. G IV    |                   |      | 0.002 (S)   |      |            |      |            |      |         |      |
| G II vs. G V     |                   |      | <0.0001 (S) |      |            |      |            |      |         |      |
| G III vs. G IV   |                   |      |             |      | 0.793 (NS) |      |            |      |         |      |
| G III vs. G V    |                   |      |             |      | 0.042 (S)  |      |            |      |         |      |
| G IV vs. G V     |                   |      |             |      |            |      | 0.323 (NS) |      |         |      |



# significant from control, \\$ significant from group II, @ significant from group III & significant from group IV

**Fig. 49:** A Histogram: illustrating mean values of Caspase 3 obtained from different groups of the examined animals.

#### 4. Discussion:

In the current study, manifestations of the pathological impact of CSA administration on the renal tissue of the examined animals were recorded in groups II, III and IV with marked histological and laboratory alterations in groups II and III. Examination of both renal cortex and medulla revealed extremely shrunken glomeruli with a widened urinary space, extensive fat degeneration, cytoplasmic vacuolation and rarefaction, exfoliation of lining

epithelial cells lost apical brush border, intra-luminal casts, with pyknotic, karyolytic nuclei, mitochondrial damage, lost apical brush microvilli, lost basal infoldings, hyaline degeneration, haemorrhage and mononuclear cell infiltration in the interstitial tissue.

In the current study, CSA administration led to decreased levels of superoxide dismutase, glutathione peroxidase, VEGF, and increased levels of renal thiobarbituric acid, caspase 3, IL1b, TGF- B1, serum creatinin and blood urea nitrogen. This was in

accordance with (29, 30) who stated that the pathogenic mechanism of chronic CsA nephrotoxicity appears to be associated with direct tubular injury or vascular injury and chronic renal ischemia, resulting in tubular atrophy and interstitial fibrosis. The damage that CsA causes to renal tubular cells and interstitium lead to elimination of renal tubular cells by apoptosis and kidney damage develops by hyperactivating immune mediators such as angiotensin II, transforming growth factor (TGF)- $\beta$  1, osteopontin (OPN) and macrophages in addition to direct toxic effects of CsA. OPN is expressed mainly in Henle's distal tubule and renal medulla loop, and normally not represented in the renal cortex. CsA administration may cause macrophage infiltration and interstitial fibrosis by increasing OPN expression in the kidneys. In the pathogenesis of glomerulosclerosis and tubulointerstitial fibrosis, TGF- $\beta$  1 is considered to be an essential cytokine and increased expression of TGF- $\beta$  1 compared to dose of CsA. An rise in TGF- $\beta$  1 by CsA is associated with tubulointerstitial fibrosis by rising the extracellular matrix and activating the RAS (31, 32, 33), rapid contact between CsA and cell organelles has been documented to be related to the chemical composition of this drug as since CsA is a highly lipophilic agent that makes it easier to bind to organelles membranes particularly mitochondria and endoplasmic reticulum, because it contains large quantities of unsaturated fatty acids and large total surface area, rendering the cells more vulnerable to oxidative stress. In addition, increased production of ROS might be due to blocking the permeability of transition pore of mitochondria resulting in an increase in the mitochondrial Ca<sup>2+</sup> level. There is also an alteration in the transport chain of mitochondrial electrons that result in oxidative phosphorylation, thereby increasing the production of ROS. Moreover, CsA is metabolized by cytochrome P-450 3A which along with the mitochondrial can also induce ROS production. They added that treatment with CsA induced a haem oxygenase-1 variance that is known to be an enzyme linked to cell redox status.

In the present work, specimens of rat kidney left for spontaneous recovery presented a limited degree of regeneration and restoration of normal histological pattern of renal tissue architecture. This was in agreement with (34, 1) who reported nephrotoxicity caused by acute or chronic CsA results in impairment of renal function and histopathological alterations. They added that histological changes resulting from CsA continue or improve even after the drug was stopped. Thus, the only way to prevent permanent renal histological changes such as tubulointerstitial fibrosis may be to avoid the usage of the medication.

In the current study, stem cell therapy markedly ameliorated the histological and laboratory alterations

exerted by CSA administration ( group IV) especially when pre-treated with erythropoietin (EPO ) ( group V). This was in agreement with (7, 1) who reported that the renoprotective effect of MSCs by releasing soluble factors was due to their paracrine actions on the injured kidney. Moreover, EPO is a glycoprotein hormone that regulates bone marrow erythropoiesis through the EPO (EpoR) receptor. Many other types of cells, including cardiomyocytes, endothelial cells, neurons, and renal tubular cells express the EpoR and respond to treatment with EPO. EPO protects against tissue injury in the kidneys. Some experimental studies in vivo and in vitro have shown that MSCs followed by incubation with EPO substantially preserved the morphological characteristics of injured renal tissue have a better restorative effect against fibrosis induced by TGF- $\beta$ 1. They added that EPO exerts this effect on stem cells via induction of a noticeable change in proliferation rate and cytoskeletal rearrangements, increased migration.

#### References:

1. Zhou, S.; Liu, Y.; Zhang, Y.; Hu, J.; Liu, D.; Chen, H.; Li, M.; Guo, Y.; Fan, L.; Li, L.Y. and Zhao, M. (2018): Bone mesenchymal stem cells pretreated with erythropoietin enhance the effect to ameliorate cyclosporine A-induced nephrotoxicity in rats. *The Journal of Cellular Biochemistry*, 119: 8220–8232.
2. Naesens, M.; Kuypers, D.R. and Sarwal, M. (2009): Calcineurin inhibitor nephrotoxicity. *Clin J Am Soc Nephrol.*, 4:481–508.
3. Korolczuk, A.; Maciejewski, M.; Smolen, A.; Dudka, J.; Czechowska, G. and Widelska, I. (2014): The role of peroxisome-proliferator-activating receptor gamma agonists: Rosiglitazone and 15-deoxy-delta12, 14-prostaglandin J2 in chronic experimental cyclosporine A-induced nephrotoxicity. *J Physiol Pharmacol.*, 65: 867–876.
4. Hewedy, W.A. and Mostafa, D.K. (2016): Nebivolol suppresses asymmetric dimethylarginine and attenuates cyclosporine-induced nephrotoxicity and endothelial dysfunction in rats. *Pharmacol Rep.*, 68:1319–1325.
5. Moghadasali, R.; Hajinasrollah, M. and Argani, H. (2015): Autologous transplantation of mesenchymal stromal cells tends to prevent progress of interstitial fibrosis in a rhesus *Macaca mulatta* monkey model of chronic kidney disease. *Cytotherapy*, 7:1495–1505.
6. Ashour, R.H.; Saad, M.A. and Sobh, M.A. (2016): Comparative study of allogenic and xenogeneic mesenchymal stem cells on

- cisplatin-induced acute kidney injury in Sprague-Dawley rats. *Stem Cell Res. Ther.*, 7:126.
7. Wang, Y.; Lu, X.; He, J. and Zhao, W. (2015): Influence of erythropoietin on microvesicles derived from mesenchymal stem cells protecting renal function of chronic kidney disease. *Stem Cell Res. Ther.*, 6:100.
  8. Squillaro, T.; Peluso, G. And Galderisi, U. (2016): Clinical trials with mesenchymal stem cells: An update. *Cell Transplant.*, 25: 829–848.
  9. Roushandeh, A.M.; Bahadori, M. and Roudkenar, M.H. (2017): Mesenchymal stem cell-based therapy as a new horizon for kidney injuries. *Arch Med. Res.*, 48:133–146.
  10. Fontaine, M.J.; Shih, H.; Schafer, R. and Pittenger, M.F. (2016): Unraveling the mesenchymal stromal cells' paracrine immunomodulatory effects. *Transfus. Med. Rev.*, 30:37–43.
  11. Li, W.; Wang, L.; Chu, X.; Cui, H. and Bian, Y. (2017): Icariin combined with human umbilical cord mesenchymal stem cells significantly improve the impaired kidney function in chronic renal failure. *Mol. Cell Biochem.*, 428:203–212.
  12. Xinaris, C.; Morigi, M. and Benedetti, V. (2013): A novel strategy to enhance mesenchymal stem cell migration capacity and promote tissue repair in an injury specific fashion. *Cell Transplant.*, 22: 423–436.
  13. Liu, N.; Wang, H.; Han, G.; Tian, J.; Hu, W. And Zhang, J. (2015): Alleviation of apoptosis of bone marrow-derived mesenchymal stem cells in the acute injured kidney by heme oxygenase-1 gene modification. *Int. J. Biochem. Cell Biol.*, 69:85–94.
  14. Lin, H.; Luo, X.; Jin, B.; Shi, H. and Gong, H. (2015): The effect of EPO gene overexpression on proliferation and migration of mouse bone marrow-derived mesenchymal stem cells. *Cell Biochem Biophys.*, 71:1365–1372.
  15. Feng, J. and Wang, W. (2017): Hypoxia pretreatment and EPO-modification enhance the protective effects of MSC on neuron-like PC12 cells in a similar way. *Biochem Biophys Res Commun.*, 482:232–238.
  16. Xiang, Y.; Piao, S.G.; Zou, H.B.; Jin, J.; Fang, M.R.; Lei, D.M.; Gao, B.H.; Yang, C.W. and Li, C. (2013): L-Carnitine protects against cyclosporine- induced pancreatic and renal injury in rats. *Transplantation Proceedings*. New York, 45: 3127- 3134.
  17. Levicar, N.; Pai, M.; Habi, N. A.; Tait, P.; Jiao, L. R.; Marley, S. B.; Davis, J.; Dazi, F.; Smadja, C.; Jansen, S. L.; Nicholls, J. P.; Apperley, J. F. and Gordon, M. Y. (2008): Long-term clinical results of autologous infusion of mobilized adult bone marrow derived CD34 cells in patients with chronic liver disease. *Cell Prolif.*, 41:115-125.
  18. Calvi, E.N.V.; Nahas, F.X.; Barbosa, M.V.; Calil, J.A.; Ihara, S.S.M.; Silva, M.S.; De Franco, M.F. and Ferreira, L.M. (2012): An experimental model for the study of collagen fibers in skeletal muscle. *Acta Cirúrgica Brasileira*, 27 (10): 681-686.
  19. Esteva, S.; Panisello, P.; Casas, M.; Torrella, J.R.; Pagés, T. and Viscor, G. (2008): Morphofunctional responses to anaemia in rat skeletal muscle. *Journal of Anatomy*, 212: 836-844.
  20. Alhadlaq, A. and Mao, J.J. (2004): Mesenchymal Stem Cells: Isolation and Therapeutics. *Stem Cells and Development*, 13:436-448.
  21. Payushina, O.V.; Domaratskaya, E. I. and Starostin V.I. (2006): Mesenchymal Stem Cells: Sources, Phenotype, and Differentiation Potential *Biology Bulletin*, 33, 1:2-18.
  22. Widyastuti, D.A.; Ristianti, M.A. and Sari, I.M. (2019): The Study of Blood Creatinin and Urea Concentration of Wistar Rats (*Rattus norvegicus*) due to Sodium Nitrite Induction. *Jurnal Ilmu Kefarmasian Indonesia*, 17 (1): 14-20.
  23. Parada, J.S.B.; Rodrigues-Santos, P.; Lopes, P.C.; Carvalho, E.; Vala, H.; Teixeira-Lemos, E.; Alves, R.; Figueiredo, A. Mota, A.; Teixeira, F. and Reis, F. (2013): Serum and Renal Tissue Markers of Nephropathy in Rats Under Immunosuppressive Therapy: Cyclosporine Versus Sirolimus. *Transplantation Proceedings*, 45, 1149–1156.
  24. Neamati, S.; Alirezaei, M.; Kheradmand, A.; Rashidipour, M. and Saki, M.R. (2013): Antioxidant enzyme activities assay and thiobarbituric acid reactive substances concentration following administration of ghrelin in the rat kidney. *International Journal of Pharmacy Teaching & Practices*, 4 (1): 451-457.
  25. Livak, K.J. and Schmittgen, T.D. (2001): Analysis of relative gene expression data using real-time quantitative PCR and the 2<sup>(-CT)</sup> method. *Methods*, 25: 402–408.
  26. Yang, L.; Liu, G.; Zhu, X.; Luo, Y.; Shang, Y. and Gu, X.L. (2019): The anti-inflammatory and antioxidant effects of leonurine hydrochloride after lipopolysaccharide challenge in broiler chicks. *Poultry Science*, 98:1648–1657.
  27. Liu, J.; Jha, P.; Lyzogubov, V.V.; Tytarenko, R.G.; Bora, N.S. and Bora, P.S. (2011): Relationship between Complement Membrane Attack Complex, Chemokine (C-C Motif) Ligand 2 (CCL2) and Vascular Endothelial Growth Factor in Mouse Model of Laser-induced

- Choroidal Neovascularization. *The Journal of Biological Chemistry*, 286( 23): 20991–21001.
28. Patel, L. and Thaker, A. (2015): The effects of A2B receptor modulators on vascular endothelial growth factor and nitric oxide axis in chronic cyclosporine nephropathy. *Journal of Pharmacology and Pharmacotherapeutics*, 6 (3): 147- 153.
  29. Naesens, M.; Kuypers, D. R. and Sarwal, M. (2009): Calcineurin inhibitor nephrotoxicity. *Clin. J. Am. Soc. Nephrol.*, 4: 481–508.
  30. Kim, J.H.; Lee, Y.H.; Lim, B.J.; Jeong, H.J.; Kim, P.K. and Shin, J. (2016): Influence of cyclosporine A on glomerular growth and the effect of mizoribine and losartan on cyclosporine nephrotoxicity in young rats. *Scientific Reports*, 6:22374.
  31. Rezzani, R. (2006). Exploring cyclosporine A-side effects and the protective roleplayed by antioxidants: The morphological and immunohistochemical studies. *Histology and Histopathology*, 21: 301–316.
  32. Ezejiofor, A. N.; Udowelle, N. A. and Orisakwe, O. E. (2017): Nephroprotective and antioxidant effect of aqueous leaf extract of *Costus Afer Ker gawl* on cyclosporin-a (Csa) induced nephrotoxicity. *Clinical Phytoscience*, 2(1): 11.
  33. Al-Khatib, Y.H.; Al-Hamdani, N.M.H. and Gumaih, H.S.A. (2019): Ameliorated and antioxidant effects of Fucoidan against cyclosporine A-induced kidney injury in rats. *The Journal of Basic and Applied Zoology*, 80:40.
  34. Yoon, H. E. & Yang, C. W. (2009): Established and newly proposed mechanisms of chronic cyclosporine nephropathy. *Korean J. Intern. Med.*, 24: 81-92.

9/3/2020